Stellar Structure

Results

- ✓ Four first-order ordinary differential equations
- ✓ Three ordinary equations
- ✓ Four boundary conditions
- ✓ Seven variables; so given M and μ, structure is determined, $R, L, T_{\text{eff}}\, T_c, P_c$, etc.

- ✓ $\mu = \mu(r)$ varies inside the star, $\mu = \mu(\mathrm{r})$; also $\mu = \mu(t)$, if $q \neq 0$
- ✓ κ is complicated; not well known even for He
- ✓ 2 BCs at center; 2 at surface; integrating the structure equations from one end, say $r = 0, m = 0, L = 0$, may not end up to meet the BCs at the other end, $r = R_*, m = M_*, L = L_*$
- ✓ Needs special techniques even for a spherical and steady star
- No time dependence (i.e., time scales of property changes >> time scales of equilibrium
- No $\boldsymbol{B}$; no $\boldsymbol{\omega}$
- Convective transport, currently with no fundamental theory, largely simplified
- μ assumed to be homogeneous
- No relativistic effects

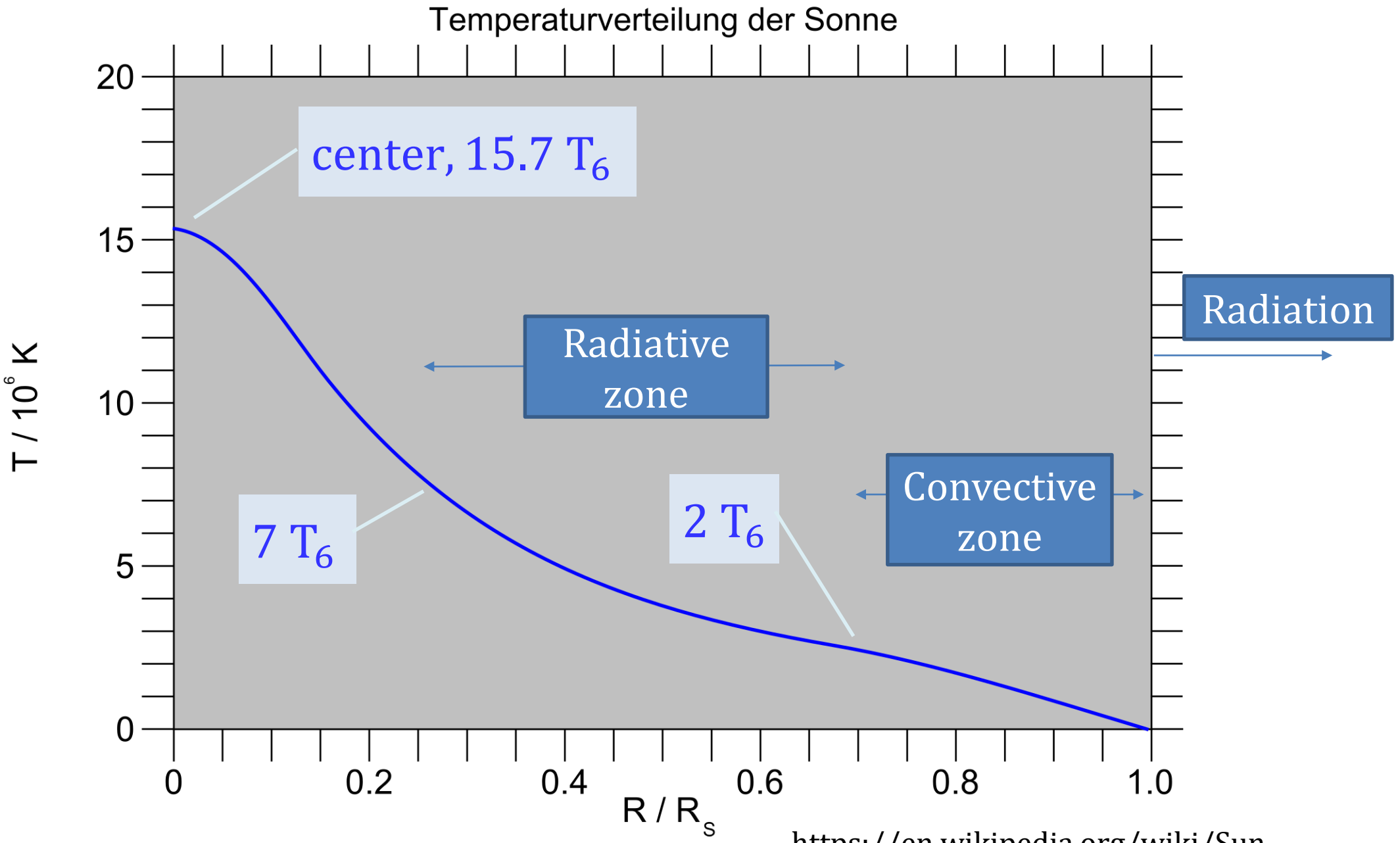

https://en.wikipedia.org/wiki/Sun

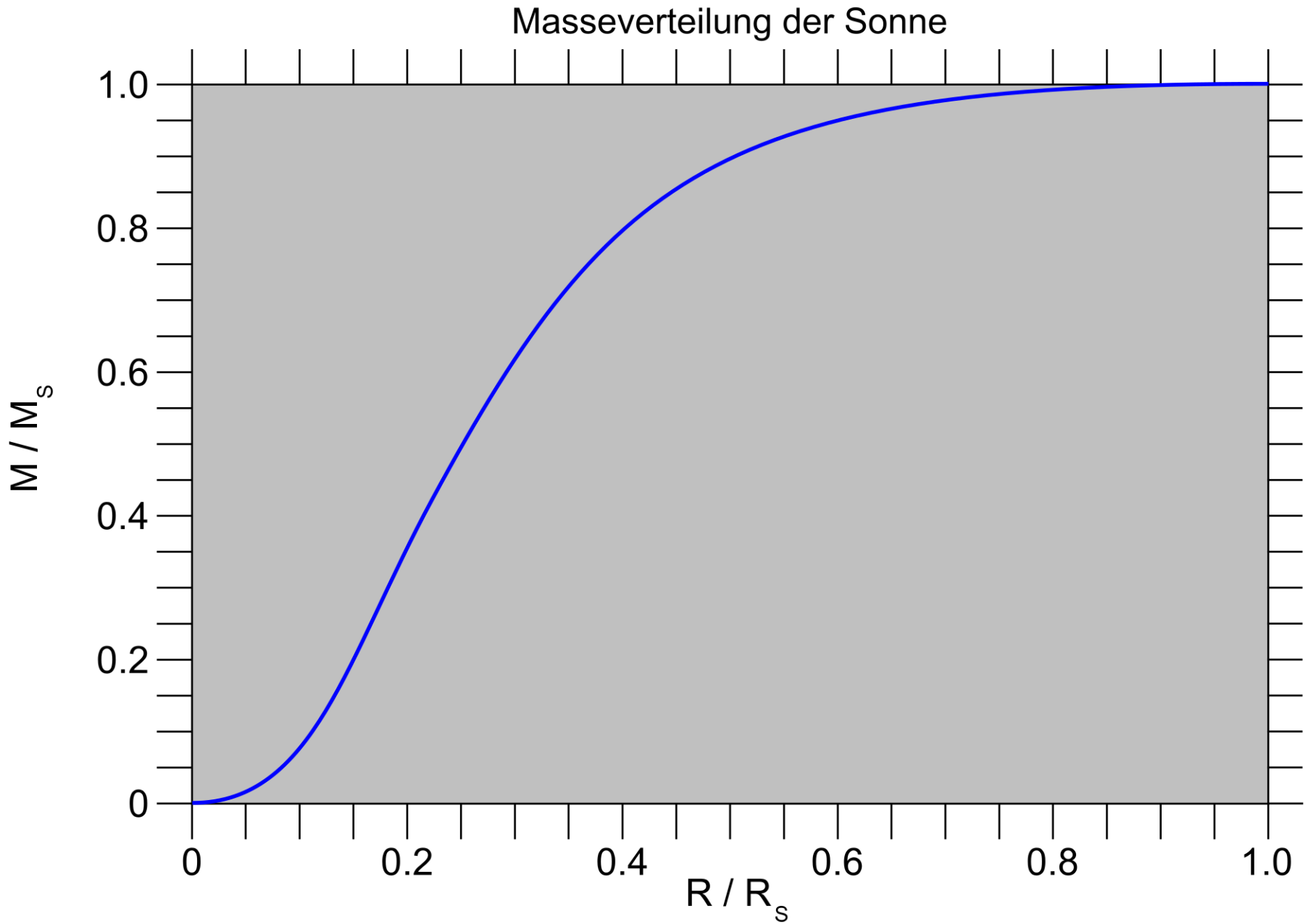
Masseverteilung der Sonne
1.0
0.8
0.6
0.4
0.2
0
M / M_S
0
0.2
0.4
0.6
0.8
1.0
R / R_S

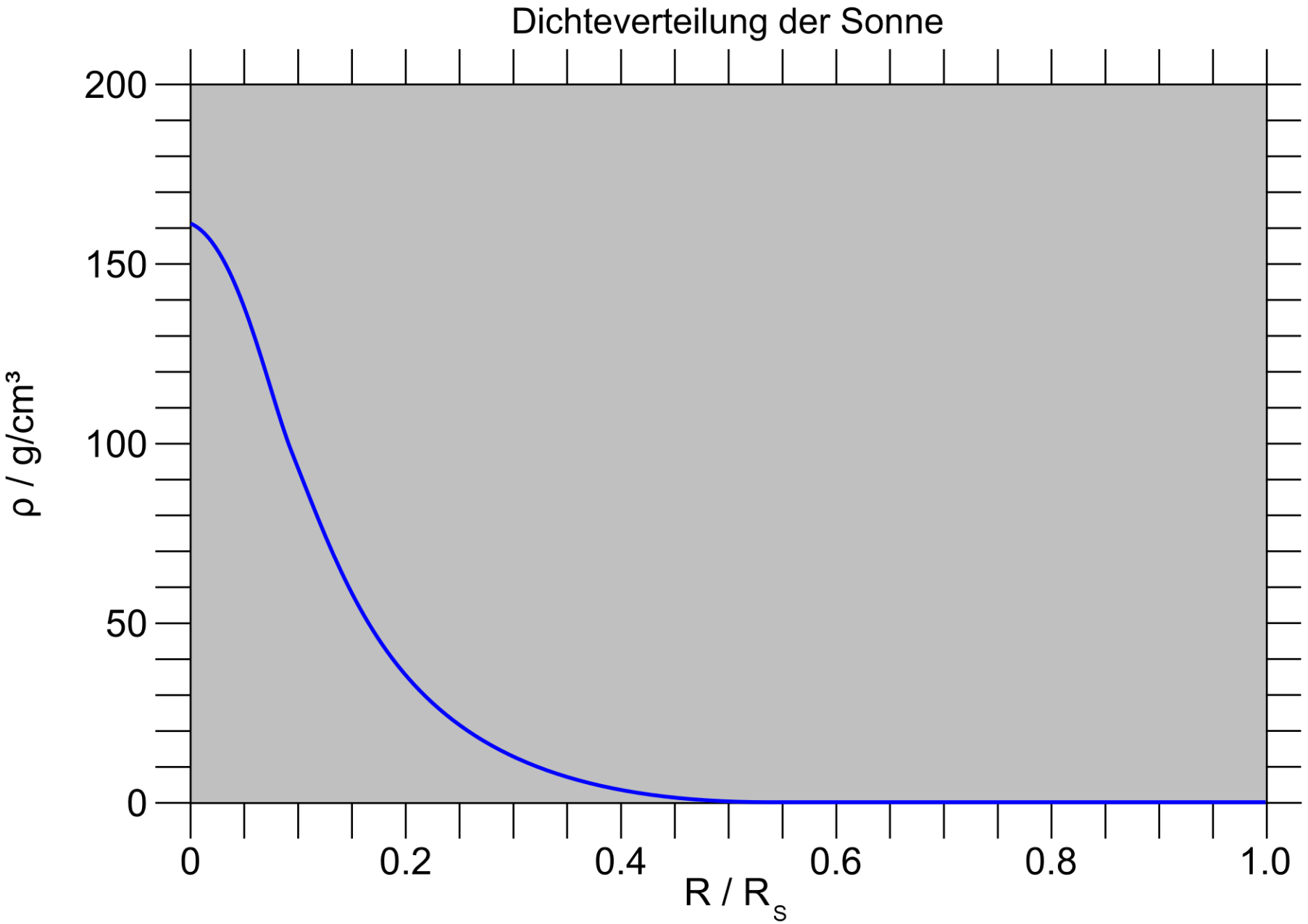
Dichteverteilung der Sonne
200
150
100
50
0
ρ / g/cm³
0
0.2
0.4
0.6
0.8
1.0
R / R_S

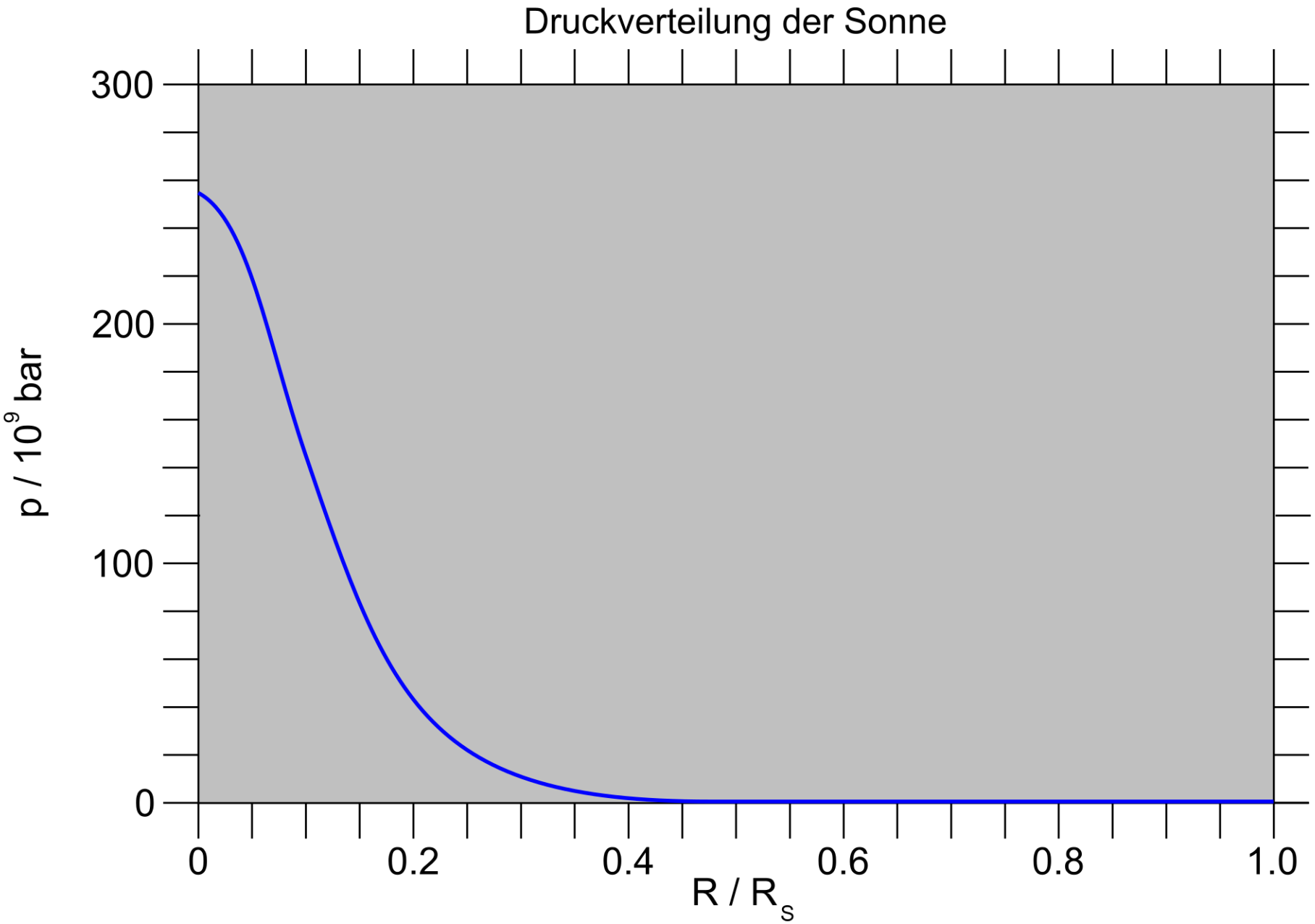
Druckverteilung der Sonne
300
200
100
0
p / 10^9 bar
0
0.2
0.4
0.6
0.8
1.0
R / R_S

Density profile --- ρ increases toward center.

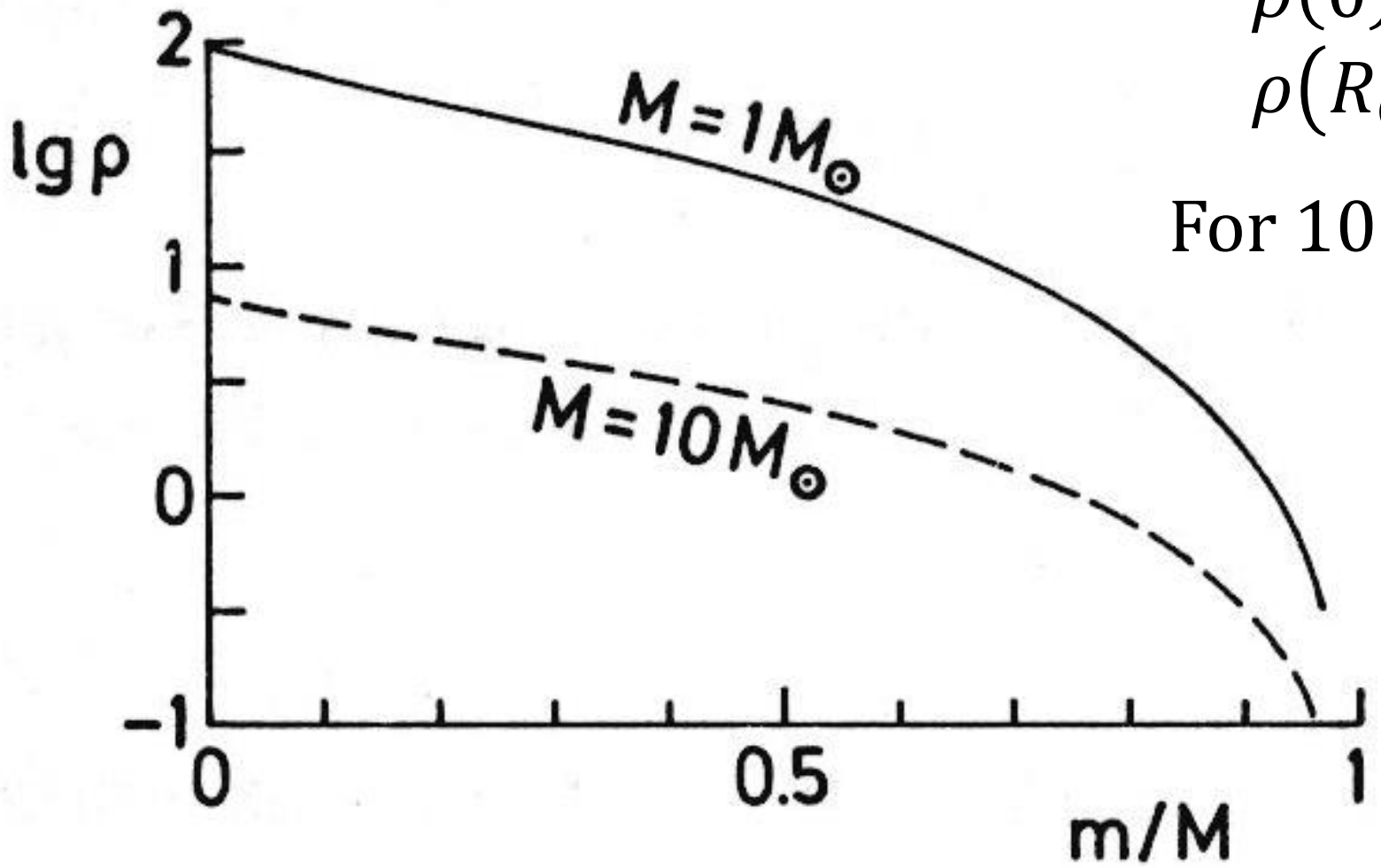

For 1 $M_\odot$,

$\rho(0) \approx 10^2\ \mathrm{g\ cm^{-3}}$

$\rho(R_\odot) \approx 10^{-7}\ \mathrm{g\ cm^{-3}}$

For 10 $M_\odot$, $\rho(0)$ 10× lower

Temperature profile --- T increases toward center.

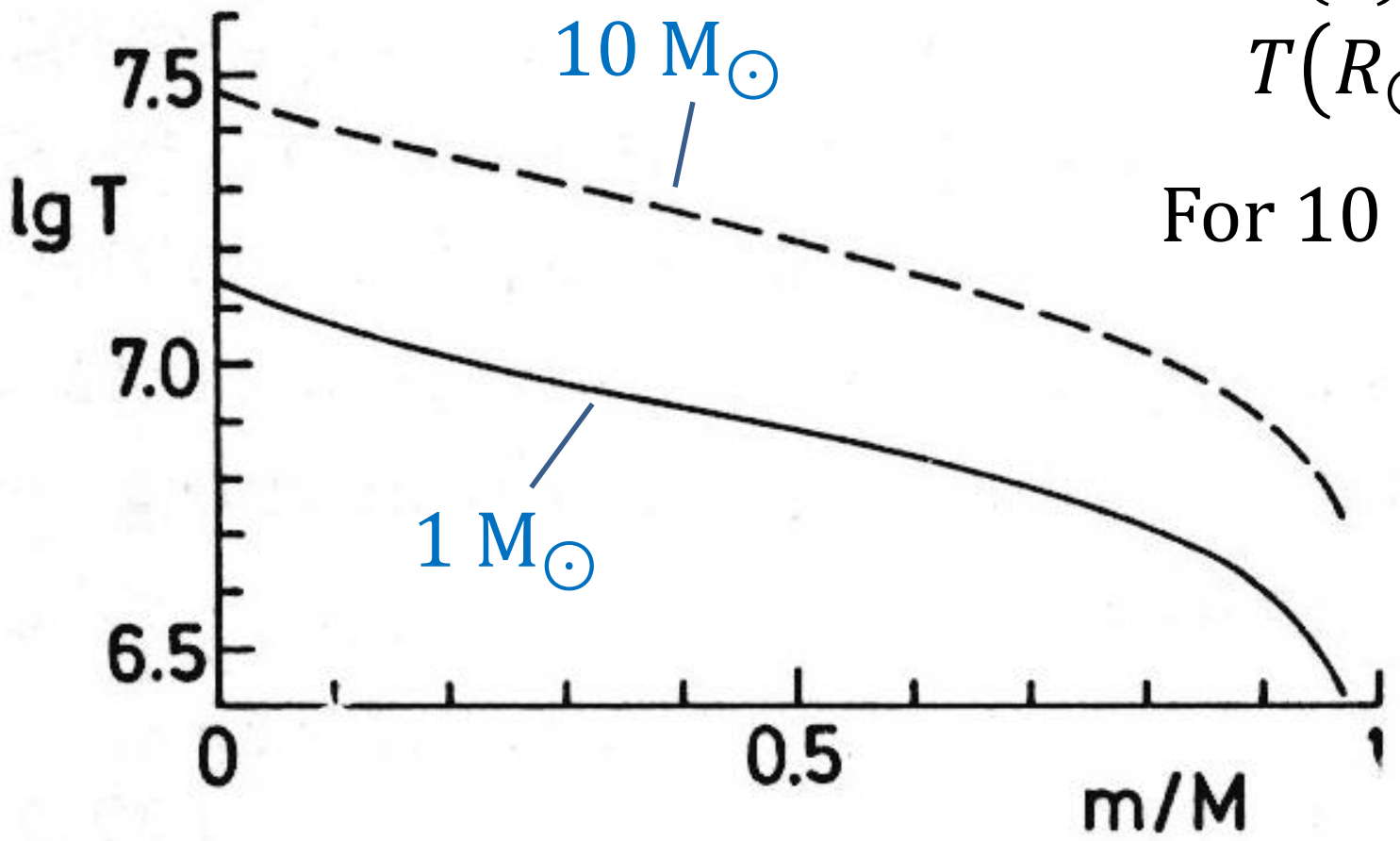

For 1 $M_\odot$,

$T(0) \approx 1.5 \times 10^7$ K

$T(R_\odot) \approx 5800$ K

For 10 $M_\odot$, $T(0) \approx 2 \times$ hotter

Massive stars at the center: (1) hotter, (2) less dense, and (3) pressure higher

Energy generation rate --- q increases toward center.

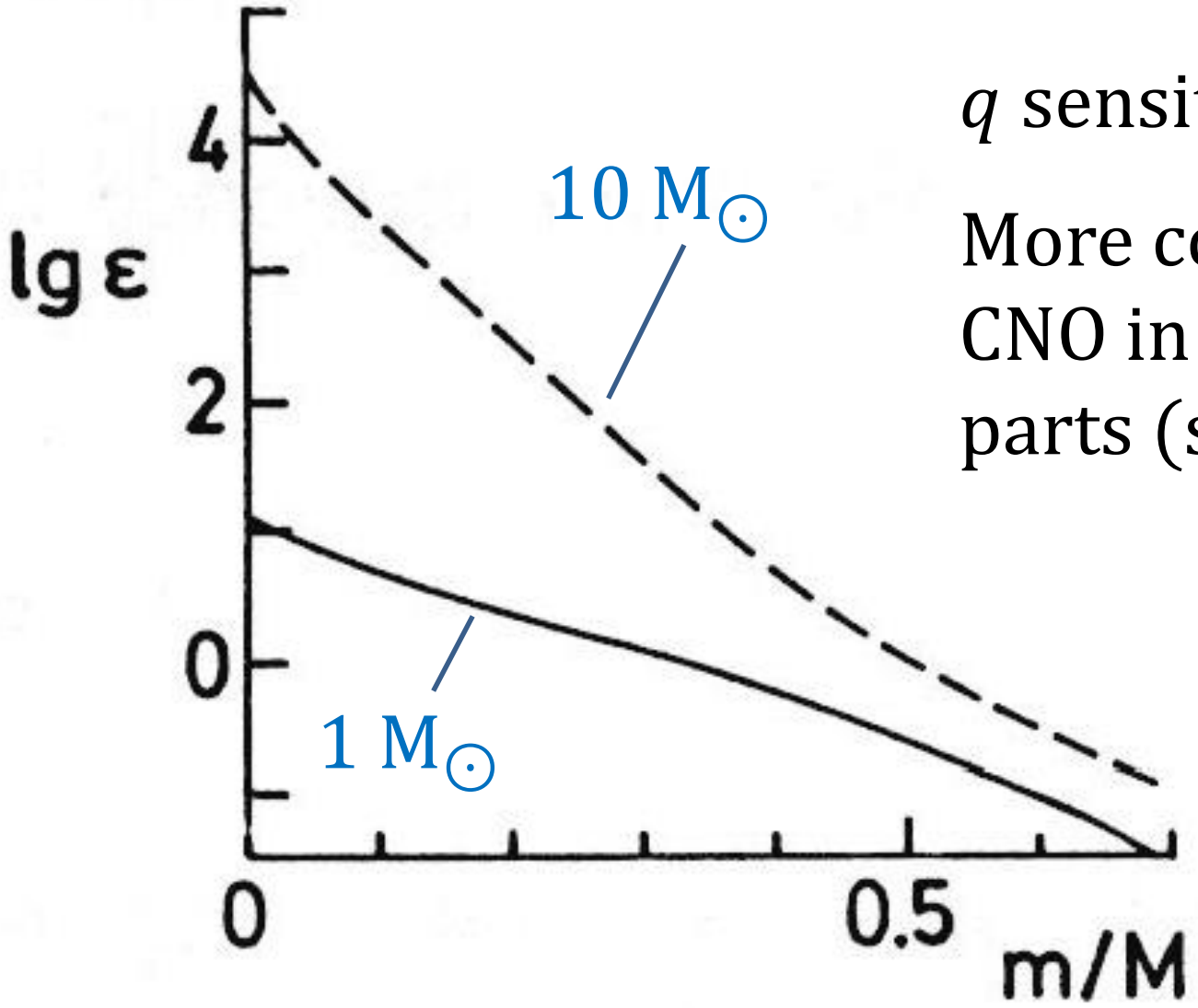

q sensitive to T $+ T$ gradient

More concentrated for higher M: CNO in the core, p-p in the outer parts (slope as in low-mass stars)

Mass-radius relation

In general, $M_* \nearrow \Rightarrow R_* \nearrow$

There is a slope break near $M_* \approx M_\odot$ because of stellar structural changes.

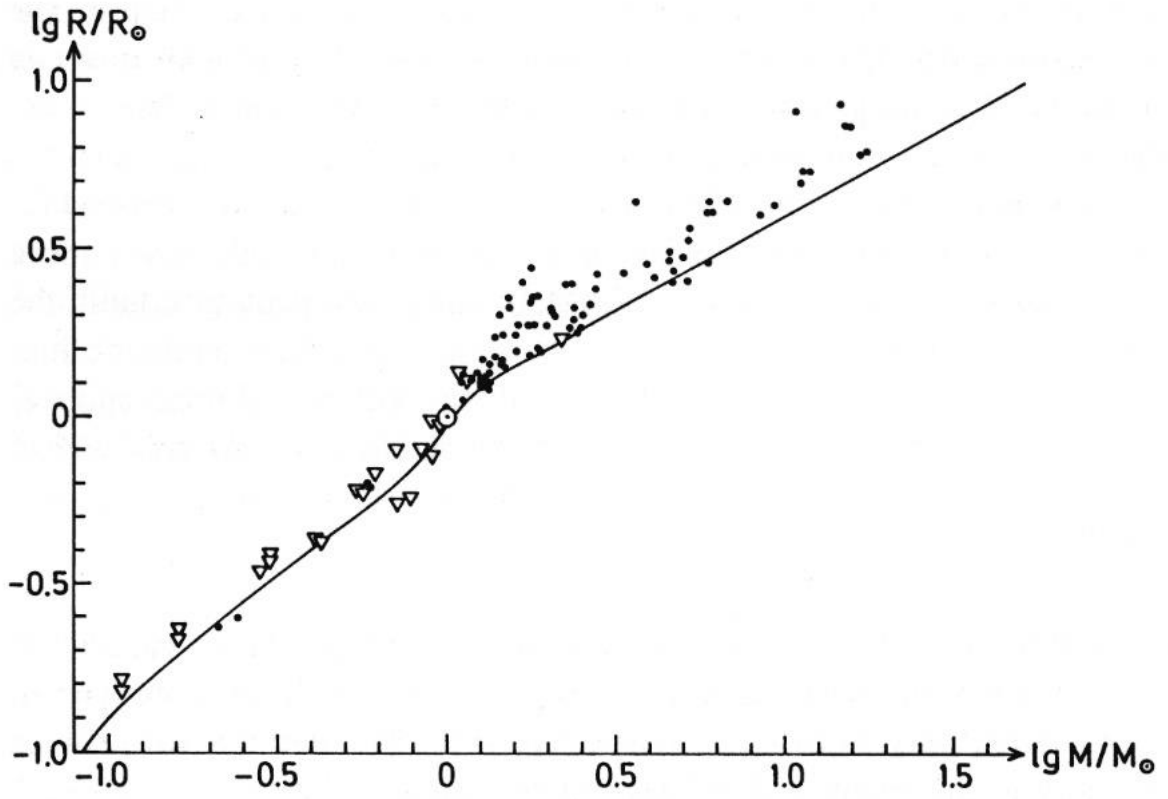

Fig. 22.2. The line shows the mass–radius relation for the models of the zero-age main sequence plotted in Fig. 22.1. For comparison, the best measurements (as selected by POPPER, 1980) of main-sequence components of detached (*dots*) and visual (*triangles*) binary systems are indicated

Kippenhahn & Weigert

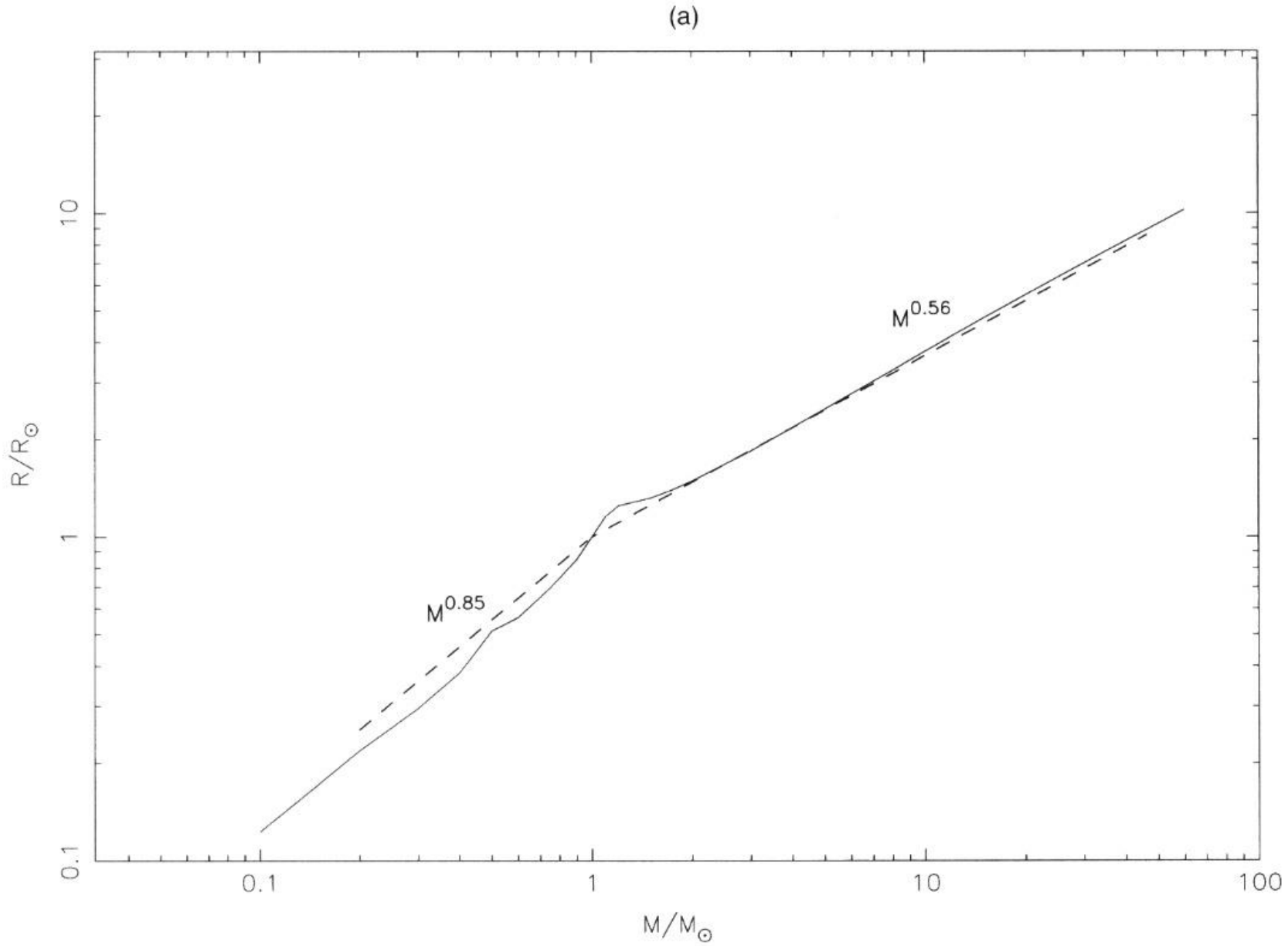

$$R \sim M^{\xi}$$

$$\xi \approx [0.6 \,..\, 0.8]$$

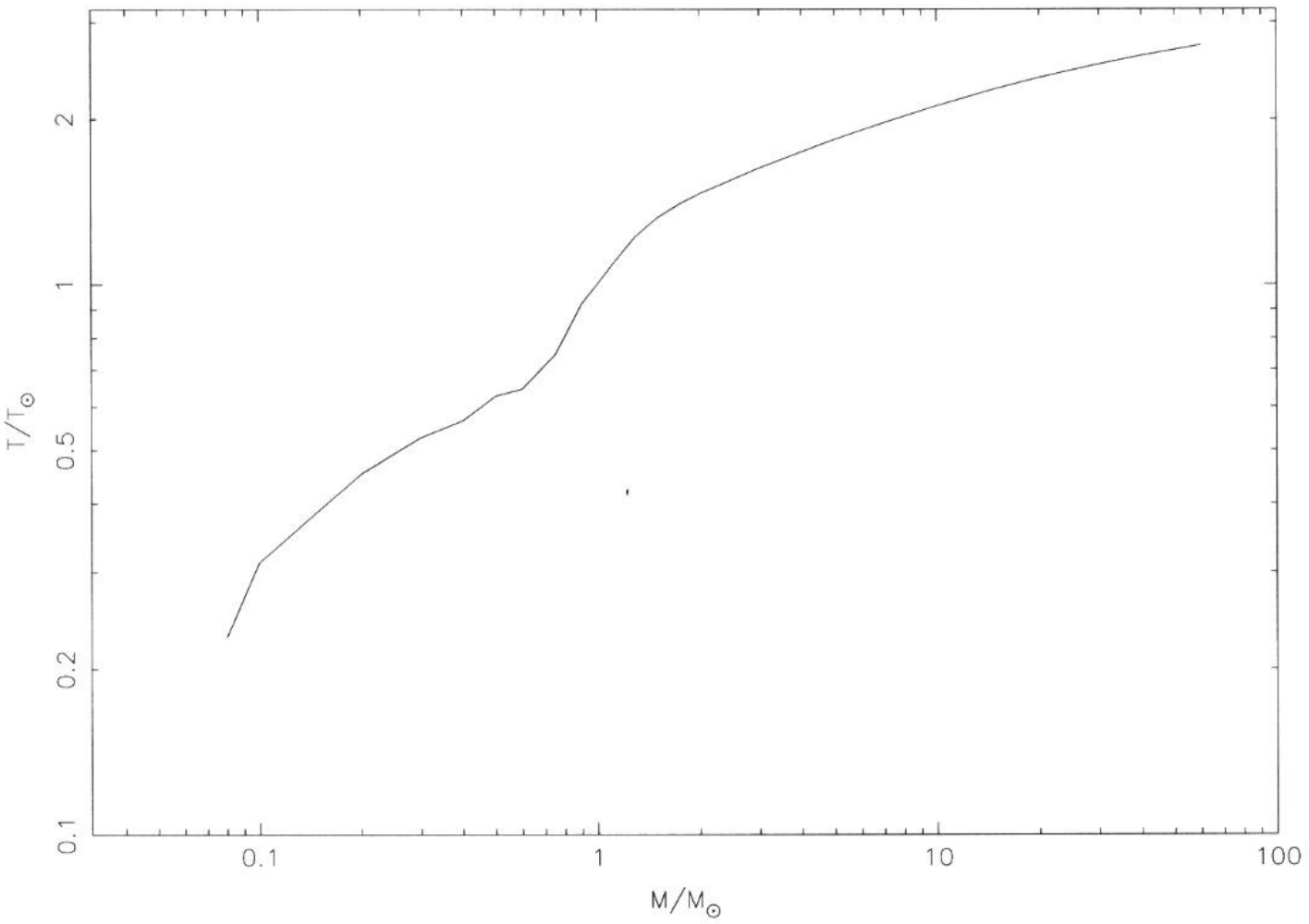

Central Temperature

$T_c \longrightarrow$ (dominant) nuclear reaction

$$T_\odot \approx 1.5 \times 10^7 \text{ K} = 15 \times 10^6 \text{ K} = 15 \text{ T}_6$$

In general, $M_* \nearrow \Rightarrow T_c \nearrow$

For $M < M_\odot, M \uparrow \Rightarrow T_c \uparrow\uparrow$

For $M > M_\odot, M \uparrow \Rightarrow T_c \uparrow$
(M 60 ×, ↑ 3↑)

- $M < 1.2\ M_{\odot}$, proton-proton chain
- $M > 1.2\ M_{\odot}$, CNO cycle → stronger T dependence
  → steeper T gradient ➔ a convective core

Mass-luminosity relation

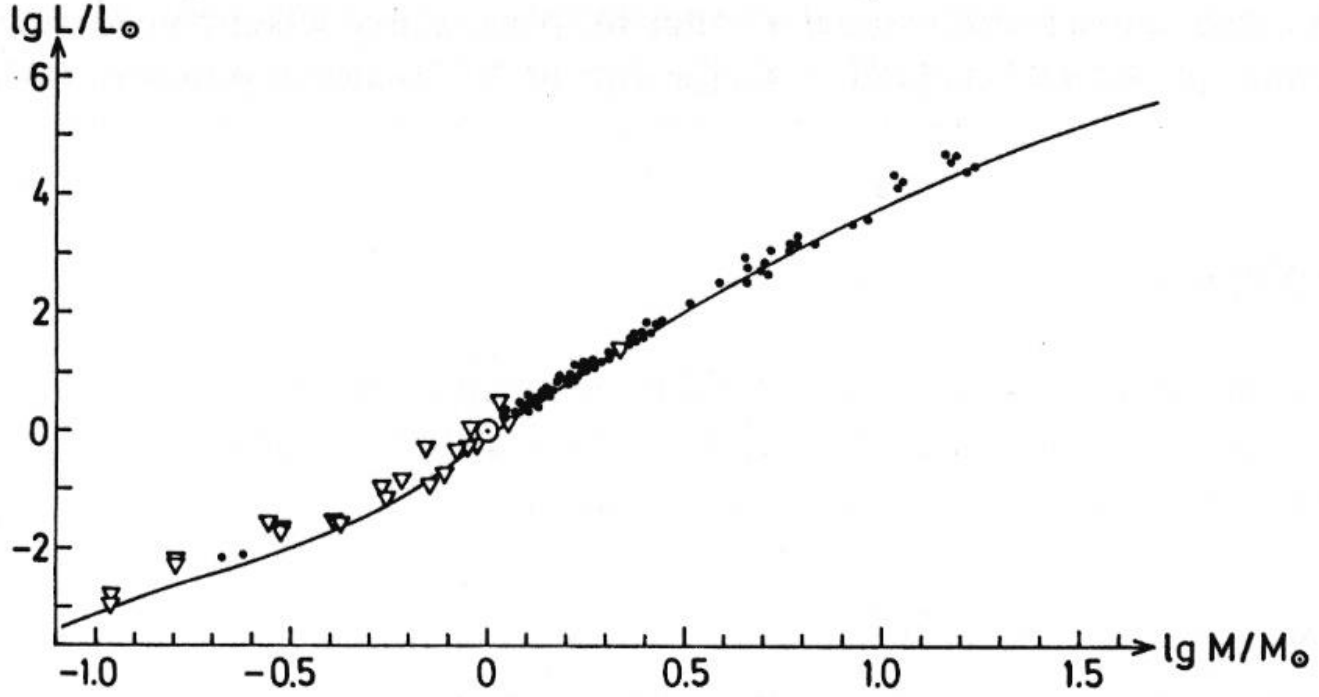

Fig. 22.3. The line gives the mass–luminosity relation for the models of the main sequence shown in Fig. 22.1. Measurements of binary systems are plotted for comparison (the symbols have the same meaning as in Fig. 22.2)

In general, $M_* \nearrow \Rightarrow L_* \nearrow$

Slope varies with respect to different mass ranges.

Overall,

$$\frac{L}{L_\odot} \approx \left(\frac{M}{M_\odot}\right)^{3.5}$$

$$\frac{L}{L_\odot} \approx 0.23 \left(\frac{M}{M_\odot}\right)^{2.3} \quad \left(\frac{M}{M_\odot} < 0.43\right)$$

$$\frac{L}{L_\odot} \approx 0.23 \left(\frac{M}{M_\odot}\right)^{4} \quad \left(0.43 < \frac{M}{M_\odot} < 2\right)$$

$$\frac{L}{L_\odot} \approx 0.23 \left(\frac{M}{M_\odot}\right)^{3.5} \quad \left(2 < \frac{M}{M_\odot} < 55\right)$$

$$\frac{L}{L_\odot} \approx 32000 \left(\frac{M}{M_\odot}\right)^{1} \quad \left(\frac{M}{M_\odot} > 55\right)$$

10^6

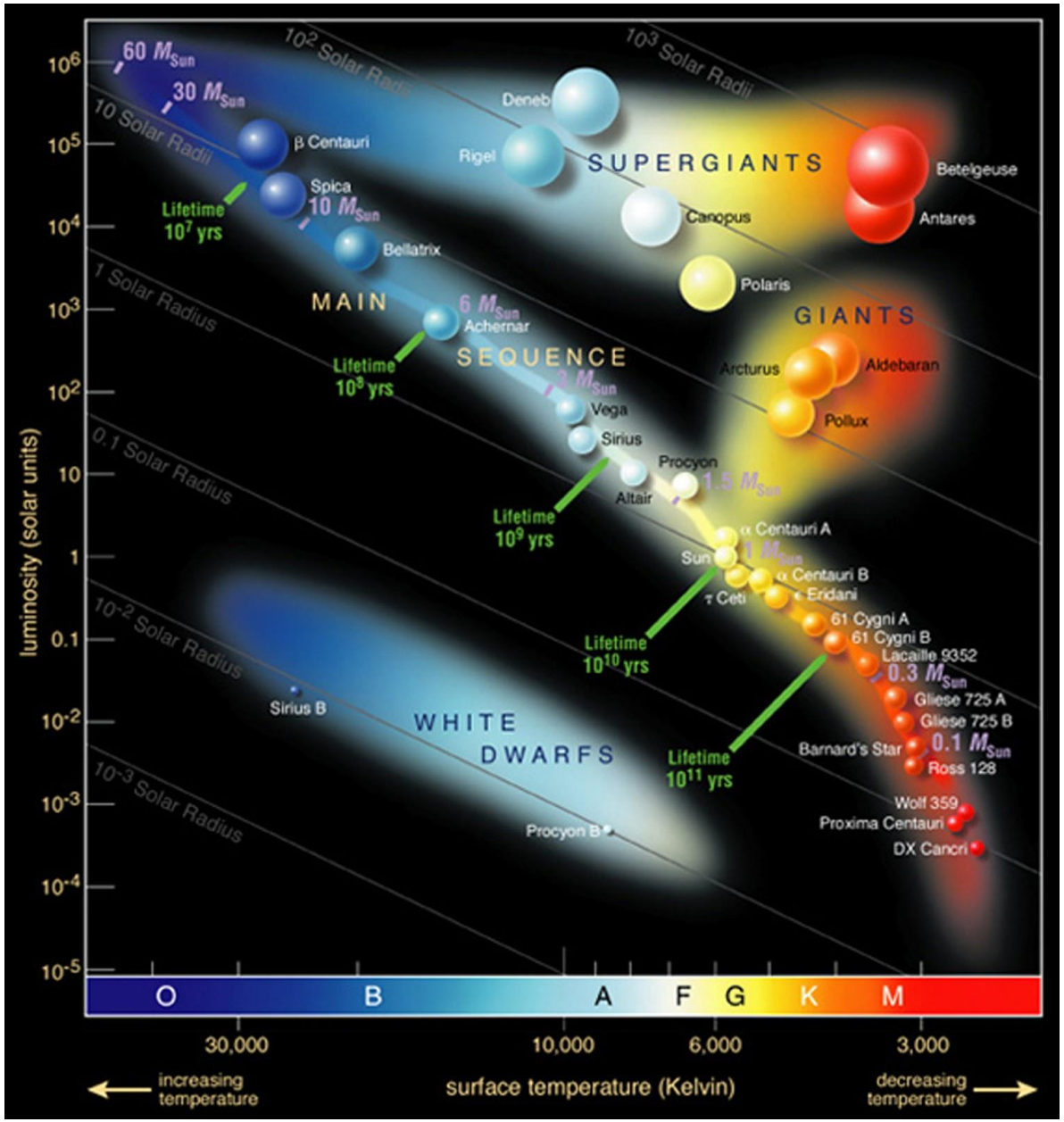

10^{-4}

30 000 K

3 000 K

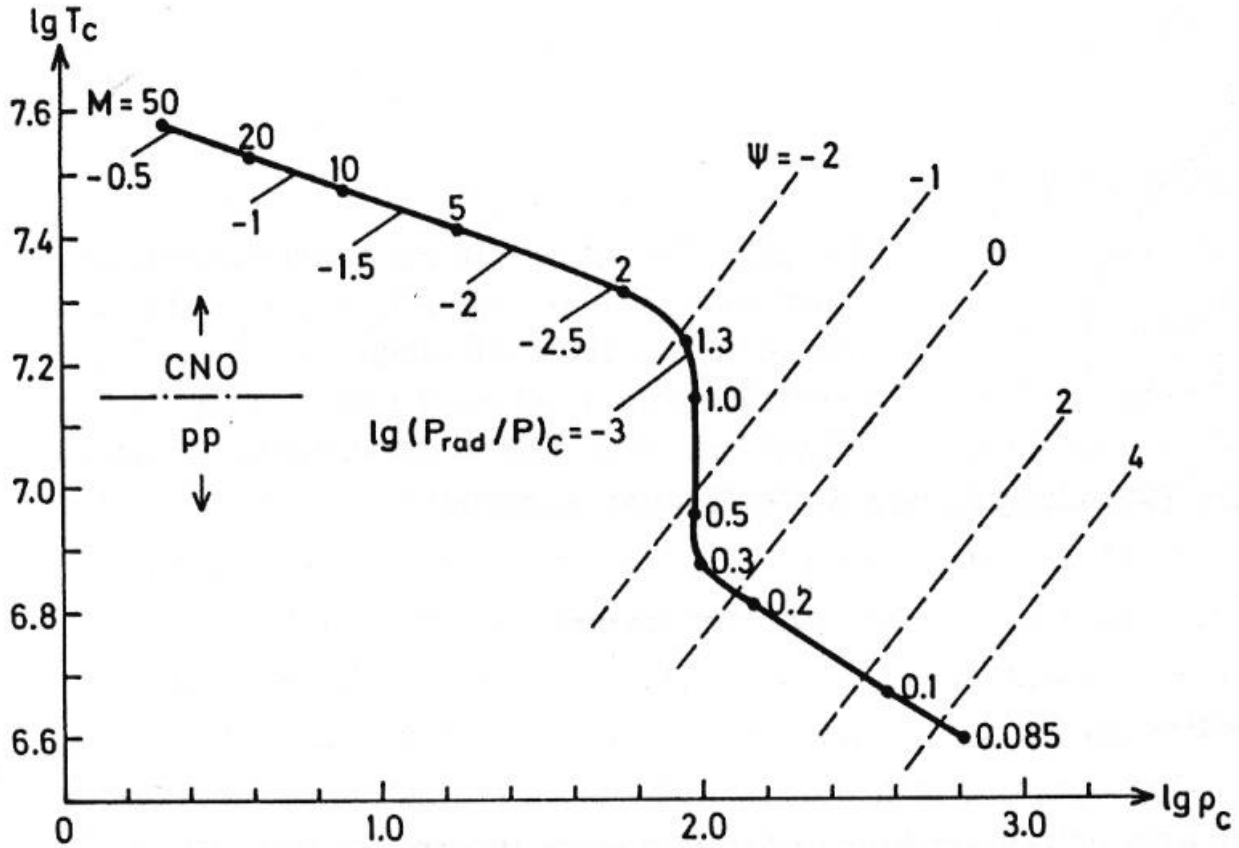

Fig. 22.5. The heavy solid line gives the central temperature T_c (in K) over the central density ϱ_c (in g cm^{-3}) for the same zero-age main-sequence models as in Fig. 22.1. The dots give the positions of some models with masses between $M = 0.085$ and $M = 50$ (in solar masses). The labels below the curve indicate the fractional contribution of the radiation pressure P_{rad} to the total pressure in the centre. The dot-dashed line at the left gives roughly the border between dominating CNO-cycle and dominating *pp*-chain reactions. The dashed lines give the constant degeneracy parameter ψ of the electron gas

Kippenhahn & Weigert

Time Scales

Different physical processes inside a star,
e.g., nuclear reactions (changing chemical composition) are slow (longer time scales); structural adjustments (dP/dt) take places on relatively shorter time scales.

- ✓ Dynamical timescale
- ✓ Thermal timescale
- ✓ Nuclear timescale
- ✓ Diffusion timescale

Dynamical Timescale

hydrostatic equilibrium $\xrightarrow{\text{perturbation}}$ motion $\xrightarrow{\text{adjustment}}$ hydrostatic equilibrium

Free-fall collapse

Equation of motion $\ddot{r} = -\frac{GM_r}{r^2} - \frac{1}{\varrho}\frac{dP}{dr}$

Near the star's surface $r = R, M_r = M$, so $\ddot{R} = -\frac{GM}{R^2} - \frac{1}{\varrho}\frac{dP}{dR}$

Free-fall means pressure $\ll$ gravity, so $\ddot{R} \approx -\frac{GM}{R^2}$

Assuming a constant acceleration $R = -\left(\ddot{R}/2\right)\tau_{\rm ff}^2$, so

$$\tau_{\rm ff} = \left(2R^3/GM\right)^{1/2} = \frac{1}{\left(\frac{2}{3}\pi G\overline{\rho}\right)^{1/2}} \approx 0.04\left(\frac{\rho_\odot}{\overline{\rho}}\right)^{1/2}\,[\mathrm{d}]$$

Stellar Pulsation

The star pulsates about the equilibrium configuration

→ same as dynamical timescale

$$\tau_{\text{pulsation}} \propto 1/\sqrt{\bar{\rho}}$$

Propagation of Sound Speed (pressure wave)

Pressure induced perturbation,

$$R/\tau_{\text{ff}}^2 = -\frac{\ddot{R}}{2} = \frac{GM}{R^2} + \frac{1}{\varrho}\frac{dP}{dR} \approx \frac{1}{\varrho}\frac{dP}{dR} \approx \frac{1}{\varrho}\frac{P}{R}$$

so $\frac{R}{\tau_{\text{ff}}} \approx \sqrt{\frac{P}{\rho}} \approx c_s$ (sound speed) $\propto \sqrt{T}$ (for ideal gas)

$$\tau_{\text{s}} \approx \frac{R}{c_s}$$

In general, $\tau_{\text{dyn}} \approx \frac{1}{\sqrt{G\bar{\rho}}} \approx \frac{1.6\times10^{15}}{\sqrt{n}}$ [s] $= 1000\sqrt{\left(\frac{R}{R_\odot}\right)^3\left(\frac{M_\odot}{M}\right)}$ [S]

Thermal Timescale

Kelvin-Helmholtz timescale (radiation by gravitational contraction)

$$E_{\text{total}} = E_{\text{grav}} + E_{\text{thermal}} = \frac{1}{2} E_{\text{grav}} = -\frac{1}{2} \alpha GM^2/R$$

This amount of energy is radiated away at a rate L, so timescale

$$\tau_{\text{KH}} = \frac{E_{\text{total}}}{L} = \frac{1}{2} \alpha GM^2/RL$$

$$= 2 \times 10^7 M^2/RL \quad [\text{yr}] \text{ in solar units}$$

$$\tau_{\text{KH}} \approx 2 \times 10^7 \left(\frac{M}{M_\odot}\right)^2 \left(\frac{R_\odot}{R}\right) \left(\frac{L_\odot}{L}\right) \quad [\text{yr}]$$

$\boldsymbol{M = 1\,\mathcal{M}_\odot, R = 1\,\mathrm{pc}}$	$\boldsymbol{M = 1\,\mathcal{M}_\odot, R = 1\,\mathcal{R}_\odot}$
$\tau_{\mathrm{dyn}} \approx 1.6 \times 10^7\ \mathrm{yr}$	$\tau_{\mathrm{dyn}} \approx 1.6 \times 10^3\ \mathrm{s} \approx 30\ \mathrm{min}$
$\tau_{\mathrm{ther}} \approx 1\ \mathrm{yr}$	$\tau_{\mathrm{ther}} \approx 3 \times 10^7\ \mathrm{yr}$

Nuclear Timescale

Time taken to radiate at a rate L on nuclear energy

$4\ {}^{1}H \rightarrow\ {}^{4}He\ (Q = 6.3 \times 10^{18}\mathrm{erg/g})$

$$\tau_{\mathrm{nuc}} = \frac{E_{\mathrm{nuc}}}{L} = 6.3 \times 10^{18}\,\frac{M}{L}$$

$$\tau_{\mathrm{nuc}} \approx 10^{11}\left(\frac{M}{M_{\odot}}\right)\left(\frac{L_{\odot}}{L}\right)\ [\mathrm{yr}]$$

From the discussion above, $\tau_{\mathrm{nuc}} \gg \tau_{\mathrm{KH}} \gg\ \tau_{\mathrm{dyn}}$

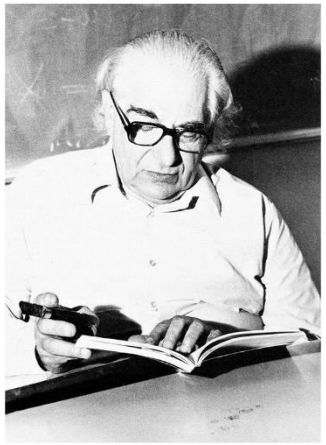

Mário Schönberg
(1914 Brazil – 1980)

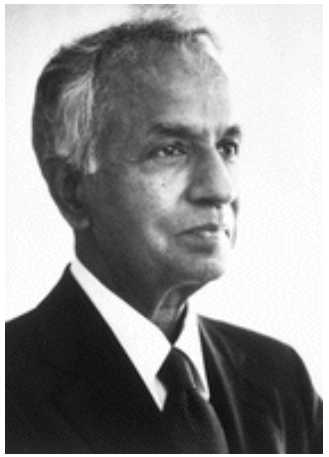

Subrahmanyan Chandrasekhar
(1910 India – 1995 USA)

The Schönberg-Chandrasekhar limit
--- the maximum mass of a fusion-less stellar core that can support against gravitational collapse

THE ASTROPHYSICAL JOURNAL

AN INTERNATIONAL REVIEW OF SPECTROSCOPY AND ASTRONOMICAL PHYSICS

VOLUME 96 SEPTEMBER 1942 NUMBER 2

ON THE EVOLUTION OF THE MAIN-SEQUENCE STARS

M. Schönberg[1] and S. Chandrasekhar

ABSTRACT

The evolution of the stars on the main sequence consequent to the gradual burning of the hydrogen in the central regions is examined. It is shown that, as a result of the decrease in the hydrogen content in these regions, the convective core (normally present in a star) eventually gives place to an isothermal core. It is further shown that there is an upper limit (~ 10 per cent) to the fraction of the total mass of hydrogen which can thus be exhausted. Some further remarks on what is to be expected beyond this point are also made.

$$\frac{M_c}{M} \approx 0.37 \left(\frac{\mu_e}{\mu_c}\right)^2$$ (~ 10-15% in reality)

Take ionized H in env ; pure He in core $\mu = 1.34$

$\mu = 0.61$

$M_c \sim 8\text{-}9\%\ M$ $\mu_c \sim 2\,\mu_e$

Beech 1988

An isothermal core cannot exceed $\sim 10\%$ of the total stellar mass, for otherwise the core cannot support the gravitational pressure of the envelope, and the core contracts.

No longer isothermal; T increases; if $\gtrsim 10^8$ K, He is ignited.

The core determines the stellar evolution (fate); the envelope follows.

Main-Sequence Lifetime of the Sun

Energy Gained in a PP Chain

- 4H → 1 He + neutrinos + energy
- Mass of 4 H = 6.693×10^{-27} kg
- − Mass of 1 He = 6.645×10^{-27} kg

Mass deficit → 0.048×10^{-27} kg = 0.7%

$$M_\odot \approx 2 \times 10^{33}\ [\mathrm{g}]$$
$$L_\odot \approx 4 \times 10^{33}\ [\mathrm{ergs/s}]$$

Fusion efficiency

Nuclear physics — **Stellar physics**

$$\tau_\odot^{\mathrm{MS}} \approx M_\odot \frac{(0.007)(0.1)\,c^2}{L_\odot} = 3.15 \times 10^{17}[\mathrm{s}] = 10^{10}\ [\mathrm{yr}]$$

Given $L_{\mathrm{MS}}/L_\odot \approx \left(M/M_\odot\right)^{3.5} \rightarrow \tau^{\mathrm{MS}} \approx 10^{10}\left(M_\odot/M\right)^{2.5}$ [yr]

Diffusion Timescale

Time taken for photons to walk out randomly from the stellar interior to eventual radiation from the surface

$$\sigma_{\text{Thomson}} = 6.6525 \times 10^{-25}\ [\text{cm}^2]$$

Thus, mean free path $\ell = 1/(\sigma_T n_e)$, where (all cgs units)
$\overline{n_e} \approx 10^{24}$ ($\bar{\rho}_\odot \approx 1.4$); $n_c \approx 10^{26}$ ($\rho_c \approx 150$). $\ell \approx [0.015 \,..\, 1.5]$ cm

Take $\ell \approx 0.3$ cm, mean-free time $\tau = (\ell/c) \approx 10^{-11}$ s

Random walk, RMS distance after N steps $d = \sqrt{N}\,\ell$.
Let $d = R_\odot \longrightarrow N \approx 5 \times 10^{22}$.
$\tau_{\text{diff}} =$ mean free time $\times$ steps $= \tau\, N \approx 10^4$ [yr]

Present Sun

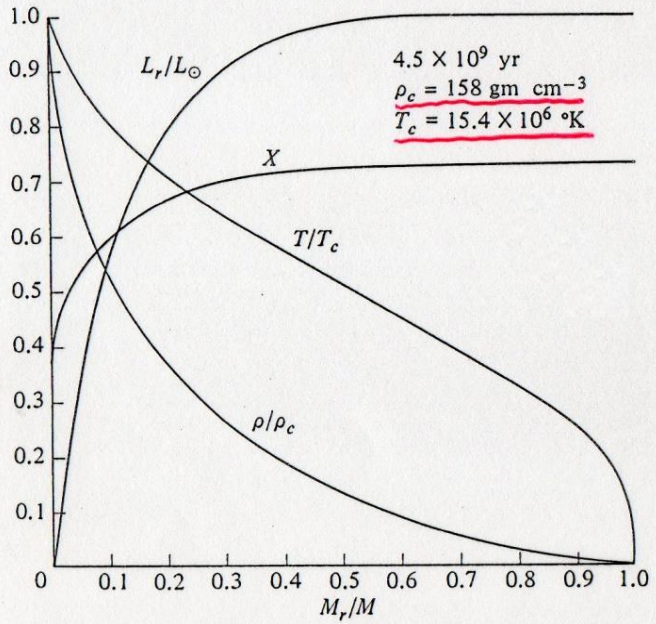

Fig. 7-11A A Model Solar Interior. Density relative to the central density ρ/ρ_c, temperature relative to central temperature T/T_c, net luminosity relative to total luminosity $L_r/L_\odot$, and hydrogen abundance X are shown as functions of fractional mass M_r/M. The chemical composition is $X = 0.730$, $Y = 0.245$, and $Z = 0.025$. The age is 4.5×10^9 years. [After S. Torres-Peimbert, E. Simpson, and R. K. Ulrich, 1969 (329).]

$X_c = 0.376$

Sun on the main sequence

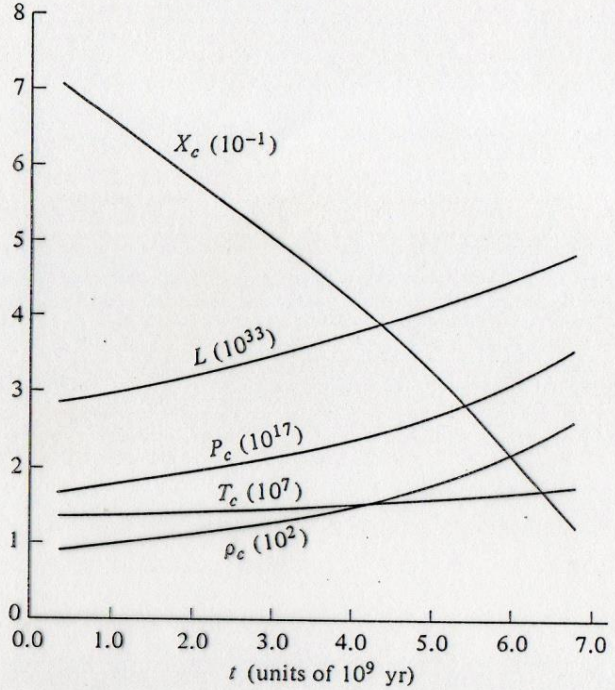

Fig. 7-11B The Evolution of the Sun during 7 Billion Years. Total luminosity L and central values of pressure P_c, temperature T_c, density ρ_c, and hydrogen abundance X_c are shown as functions of time t, which is measured from the initial (homogeneous) state for which the composition is $X = 0.730$, $Y = 0.245$, and $Z = 0.025$. The power of ten by which each value must be multiplied is indicated in parentheses. The values of P_c, ρ_c, and L are expressed in cgs units, and T_c is expressed in degrees Kelvin. [After S. Torres-Peimbert, E. Simpson, and R. K. Ulrich, 1969 (329).]

At ZAMS, X is homogeneous.

$P_{deg} \sim 0.017\, P_{total}$ at ZAMS

0.075

9.2×10^9 yr

(Fig 7-10B)

Phase Diagram of Water

$\rho - T$ diagram

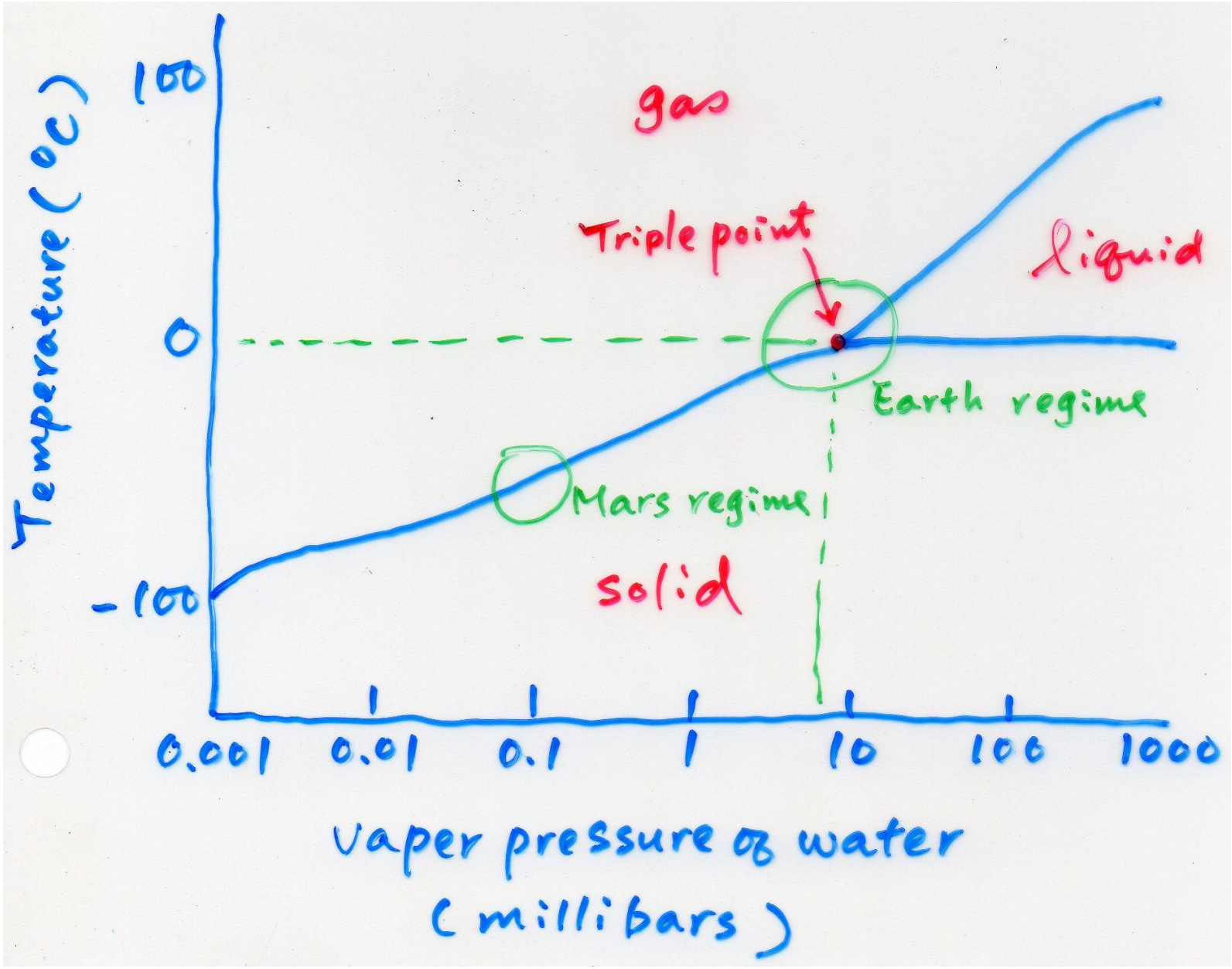

$$P_{\text{ideal gas}} \propto \rho\, T/\mu$$

$$P_{e,deg}^{NR} = 1.00 \times 10^{13} \left(\frac{\rho}{\mu_e}\right)^{5/3} \text{ [cgs]}$$

$$P_{e,deg}^{ER} = 1.24 \times 10^{15} \left(\frac{\rho}{\mu_e}\right)^{4/3} \text{ [cgs]}$$

$$P_{\text{rad}} = \frac{1}{3}\, a\, T^4$$

Non-Relativistic, Non-Degenerate (i.e., ideal gas)

Non-Relativistic, Extremely Degenerate

Extremely Relativistic, Extremely Degenerate

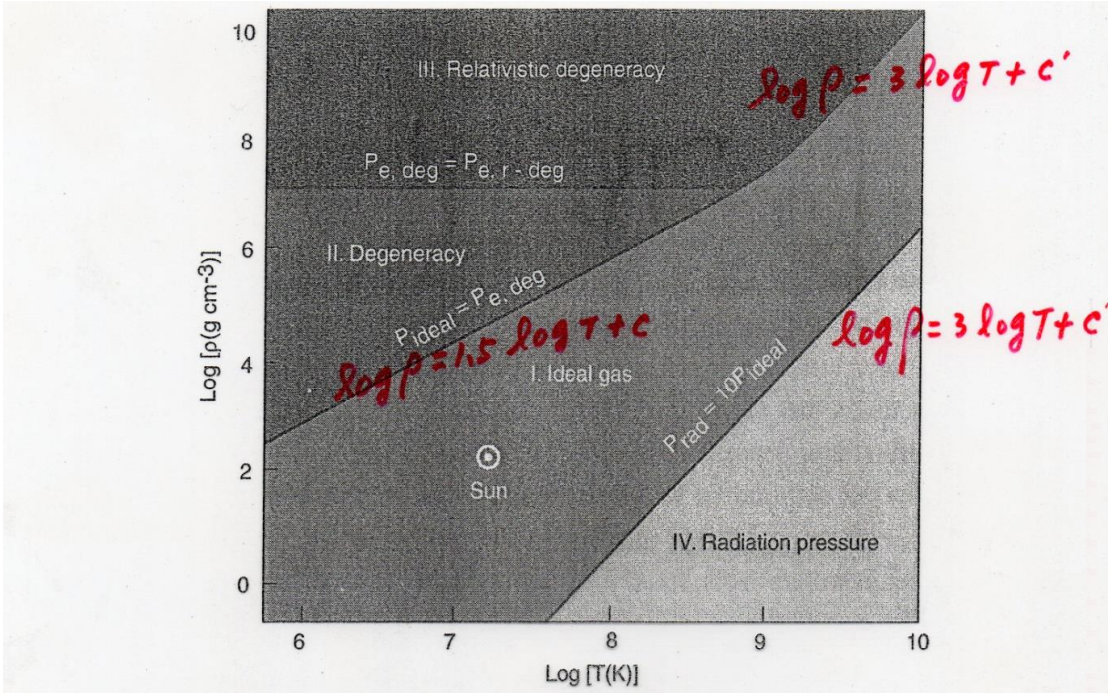

Figure 7.1 Mapping of the temperature-density diagram according to the equation of state.

NR, ND $P \sim \rho T$

NR, ED $P \sim \rho^{5/3}$

$\log \rho = 1.5 \log T + \text{const.}$

ER, ED $P \sim \rho^{4/3}$ $(\sim \rho T)$

$\log \rho = 3 \log T + \text{const}$

Prad vs Pideal gas $P_{rad} \sim T^4$, $P_{gas} \sim \rho T$

$\log \rho = 3 \log T + \text{const}$

$\log \rho = 1.5 \log T + \text{const}$

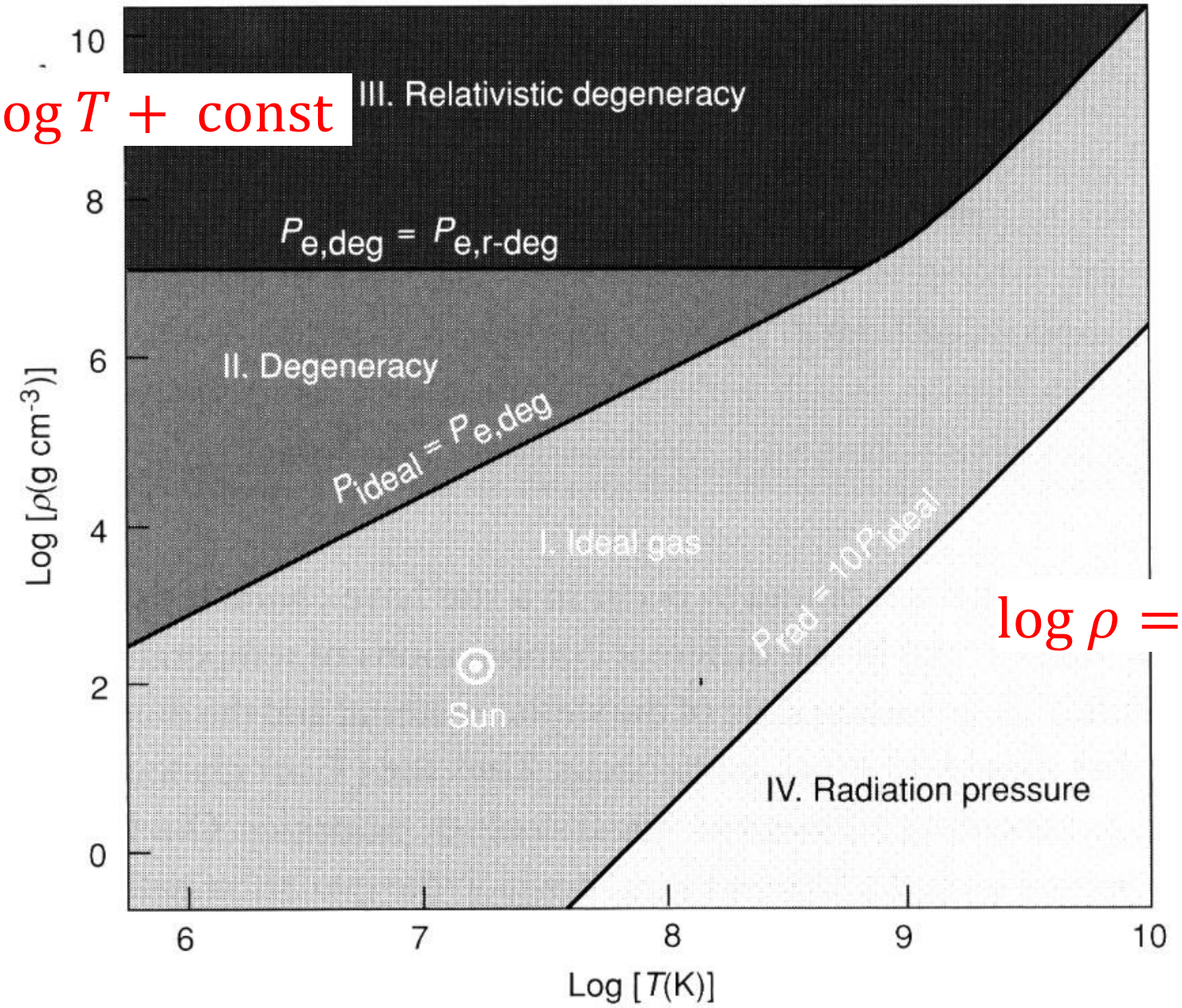

$\log \rho = 3 \log T + \text{const}$

Radiation Pressure versus Gas Pressure

$P_{\rm gas} \propto$ T balances self-gravitation OK; but $P_{\rm rad} \propto T^4$, so as stellar $M \nearrow$, $\mathrm{T_c} \nearrow \Longrightarrow P_{\rm rad} \nearrow\nearrow$

$P_{\rm rad}$ plays a more important role in more massive stars.

$P_{\rm rad} \approx P_{\rm gas}$ around 5 $\mathrm{M}_\odot$

$\Longrightarrow$ A limit when $P_{\rm rad}$ predominates

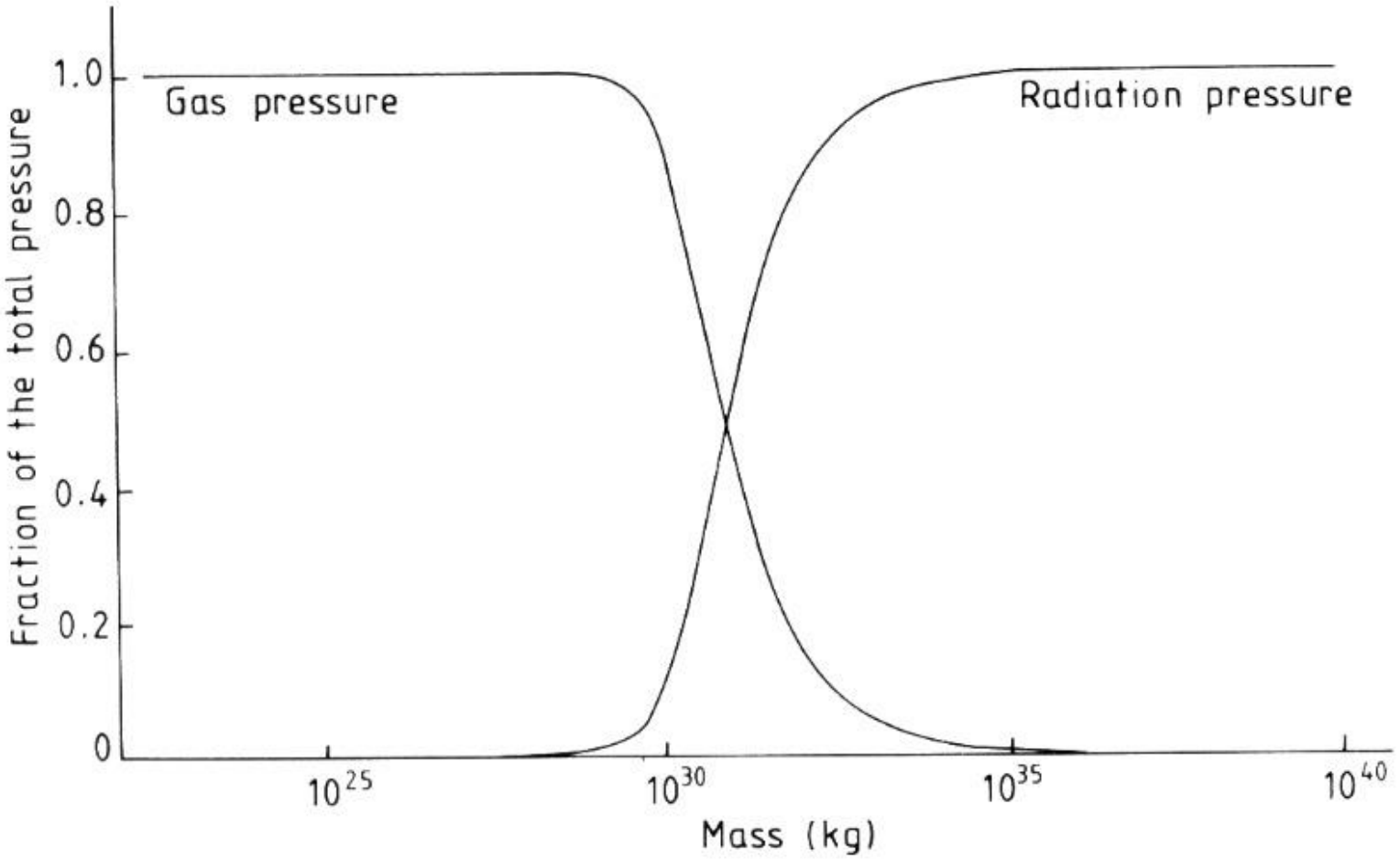

Eddington (1930)

Maximum Radiation Pressure

$$L < L_{\mathrm{Edd}} = \frac{4\pi cGM}{\kappa} = \frac{4\pi cGMm_p}{\sigma_T} \text{ (assuming ionized H)}$$

$$\approx 3.2 \times 10^4 \left(\frac{M_*}{M_\odot}\right) [L_\odot] = 1.26 \times 10^{38} \left(\frac{M_*}{M_\odot}\right) [\mathrm{erg/s}]$$

This is the **Eddington limit.**

If $L > L_{\mathrm{Edd}}$ → hydrostatic equilibrium is violated
→ super-Eddington luminosity → stellar wind

Stellar Mass Upper Limits

$L \sim M^3$

$$\frac{L_{\rm Edd}}{L_\odot} = \frac{1.26\times10^{38}}{4\times10^{33}}\left(\frac{L_*}{L_\odot}\right)^{1/3} \rightarrow L_* \sim 5\times10^6\ {\rm L}_\odot \rightarrow M_*^{\rm max} \approx 170\ M_\odot$$

Observationally, there seems indeed a limit,

e.g., Eta Carina, $\sim 150 \pm 50\ M_\odot$

$$L_{\rm Edd} \leftrightarrow \kappa, \qquad \text{so } L_{\rm Edd}^{\rm Pop\ I} < L_{\rm Edd}^{\rm Pop\ II} < L_{\rm Edd}^{\rm Pop\ III} (\approx 300\ {\rm M}_\odot)$$

Stellar Mass Lower Limits

$$q_{PP} \propto \exp\left[-33.8\, T_6^{-1/3}\right]$$

Highly sensitive to temperature.

Below about at 5 T_6, the rate becomes too low to supply energy (recall the Gamow peak).

This corresponds to about 0.1 $M_\odot$;
more precise modeling leads to $\approx 0.08\ M_\odot$.

There could be stars in which only the first two stages of the p-p chain occur, so the stars will accumulate $^3_2$He in the interior.

Stars have masses ranging from ~0.1 to ~100 solar masses.

Other Main Sequences

He MS = He stars

For H MS mixed gas, $\mu \approx 0.62$.
For He stars, $\mu \approx 1.34$

Recall for low-mass stars

$$L \sim \mu^{7.5}$$

$$L \sim \mu^{7.5} G^{7.5} M^{5.5} R^{-0.5}$$

and for massive stars

$$L \sim \mu^{4}$$

So $\log(L_{He}/L_{H}) \approx [2.5..1.33]$

For C MS, $\log(L_{C}/L_{He}) \approx 0.5$

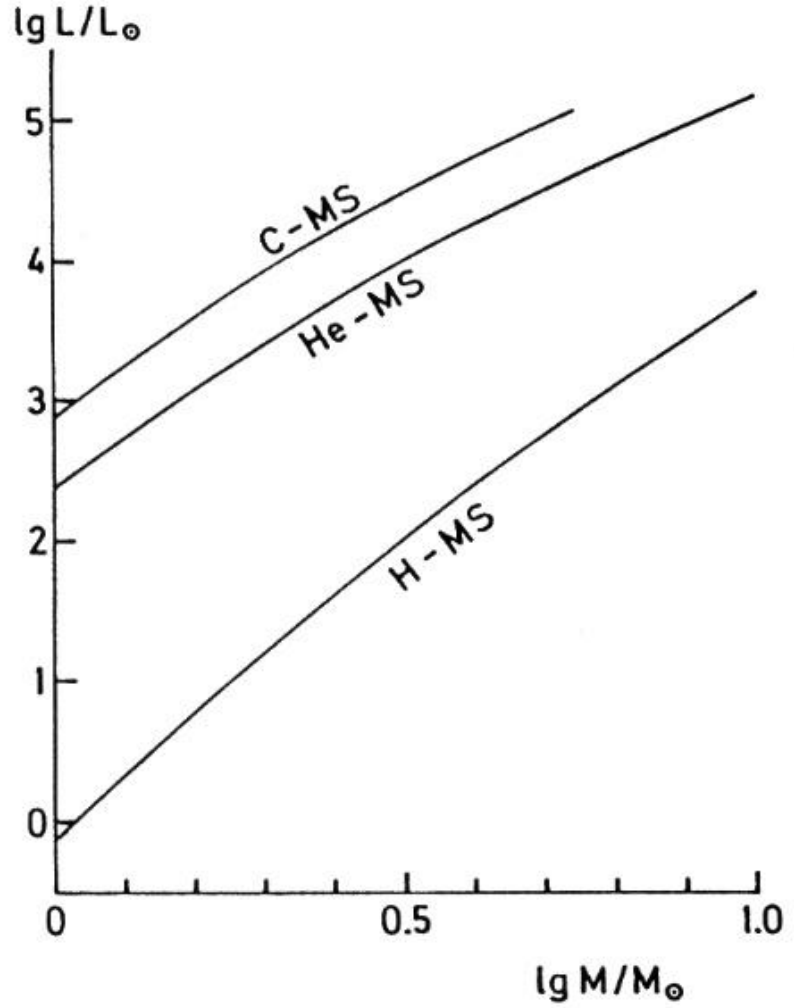

Fig. 23.2. Mass–luminosity relations for the models of the hydrogen, helium, and carbon main sequences of Fig. 23.1

Kippenhahn & Weigert

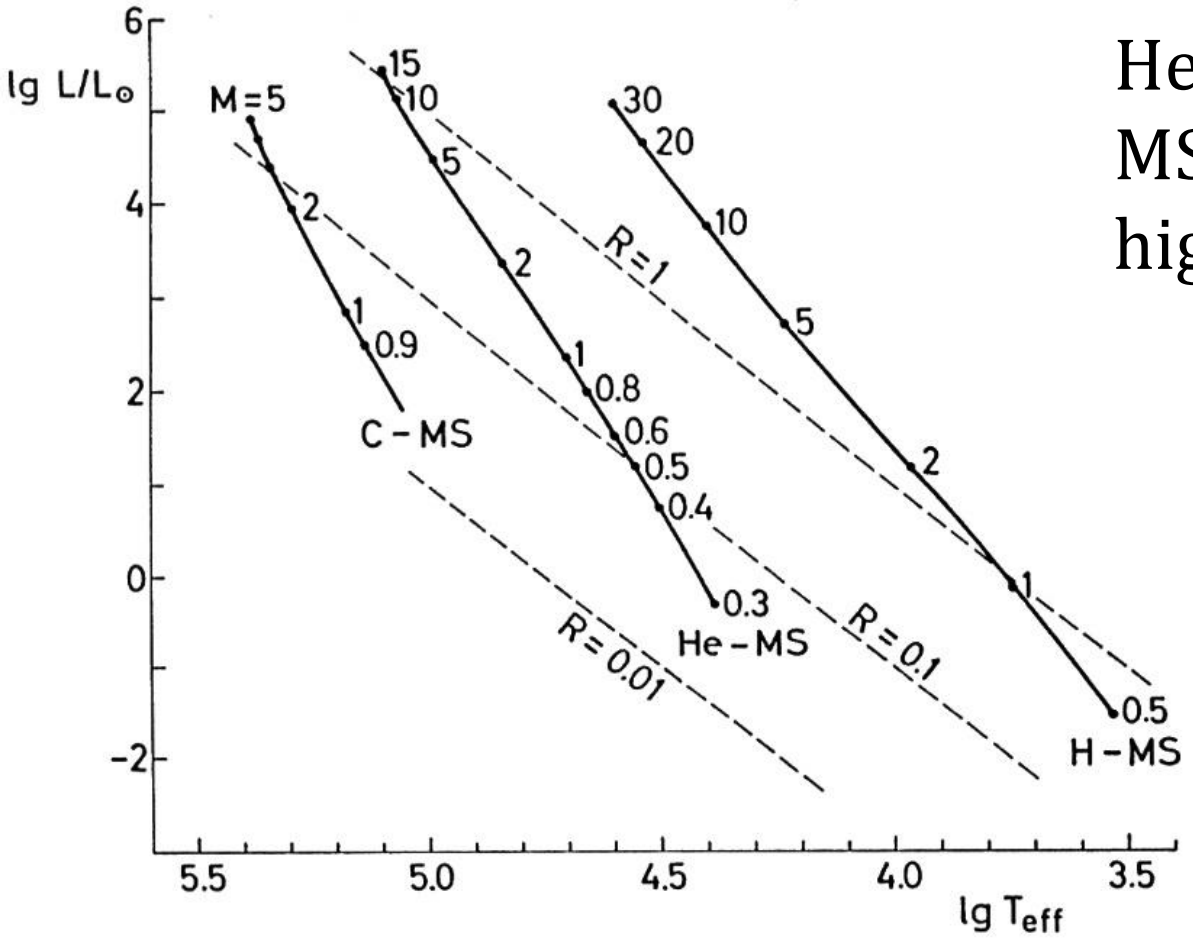

Fig. 23.1. In the Hertzsprung–Russell diagram the solid lines show the normal hydrogen main sequence (H-MS; $X_H = 0.685$, $X_{He} = 0.294$), the helium main sequence (He-MS; $X_H = 0$, $X_{He} = 0.979$) and the carbon main sequence (C-MS; $X_H = X_{He} = 0$, $X_C = X_O = 0.497$). The labels along the sequences give stellar masses M (in units of $M_\odot$). Three lines of constant stellar radius (R in units of $R_\odot$) are plotted (*dashed*)

He-MS to the far left of the H-MS, stars smaller but at higher luminosities.

Kippenhahn & Weigert

Stellar Evolution in a Nutshell

- $M \lesssim 0.5\ \mathrm{M}_\odot \longrightarrow$ fully convective
- $0.5\ \mathrm{M}_\odot \lesssim M \lesssim 2.25\ \mathrm{M}_\odot$
  $\longrightarrow$ RG + (He flash) He core $\longrightarrow$ AGB + CO core
  $\longrightarrow$ PN ejection + CO WD ($0.55\ \mathrm{M}_\odot$)
- $2.25\ \mathrm{M}_\odot \lesssim M \lesssim 10.5\ \mathrm{M}_\odot \longrightarrow$ He ignition in ND condition
  - ✓ $M \lesssim 8.5\ \mathrm{M}_\odot \longrightarrow$ CO WD ($< 1.1\ \mathrm{M}_\odot$)
  - ✓ $8.5\ \mathrm{M}_\odot \lesssim M \lesssim 10.5\ \mathrm{M}_\odot \longrightarrow$ electron deg O and Ne core
    $\longrightarrow$ AGB + ONe WD ($[1.1\ ..\ 1.37]\ \mathrm{M}_\odot$)

Iben

Effect of Rotation

Flattening $f = (a - b)/a$
(Ellipticity or oblateness)
↔ density and (balance between gravitation force and centrifugal force)

cf, eccentricity $e = \left(1 - \frac{b^2}{a^2}\right)^{1/2}$

a: semimajor axis; b: seminor axis

b/a: compression factor; aspect ratio

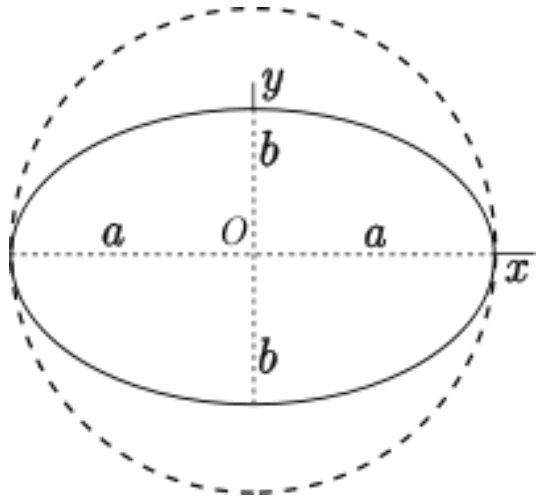

Jupiter: $1/16 \approx 6\%$
Saturn: $1/10$
Sun: $1/100000$
Moon: $1/900$
Earth: $3/1000$ ($D_{\text{eqatorial}}$ 42 km more than D_{polar}; bulge)

Solar Rotation

The Sun rotates slowly, ≈ 2 km s^{-1}@equator ($P \sim 25$ d); slower at higher latitudes ($P \sim 34$ d at poles).

Differential rotation in the convective region; rigid rotation in the radiative region (within 0.7 $R_\odot$)

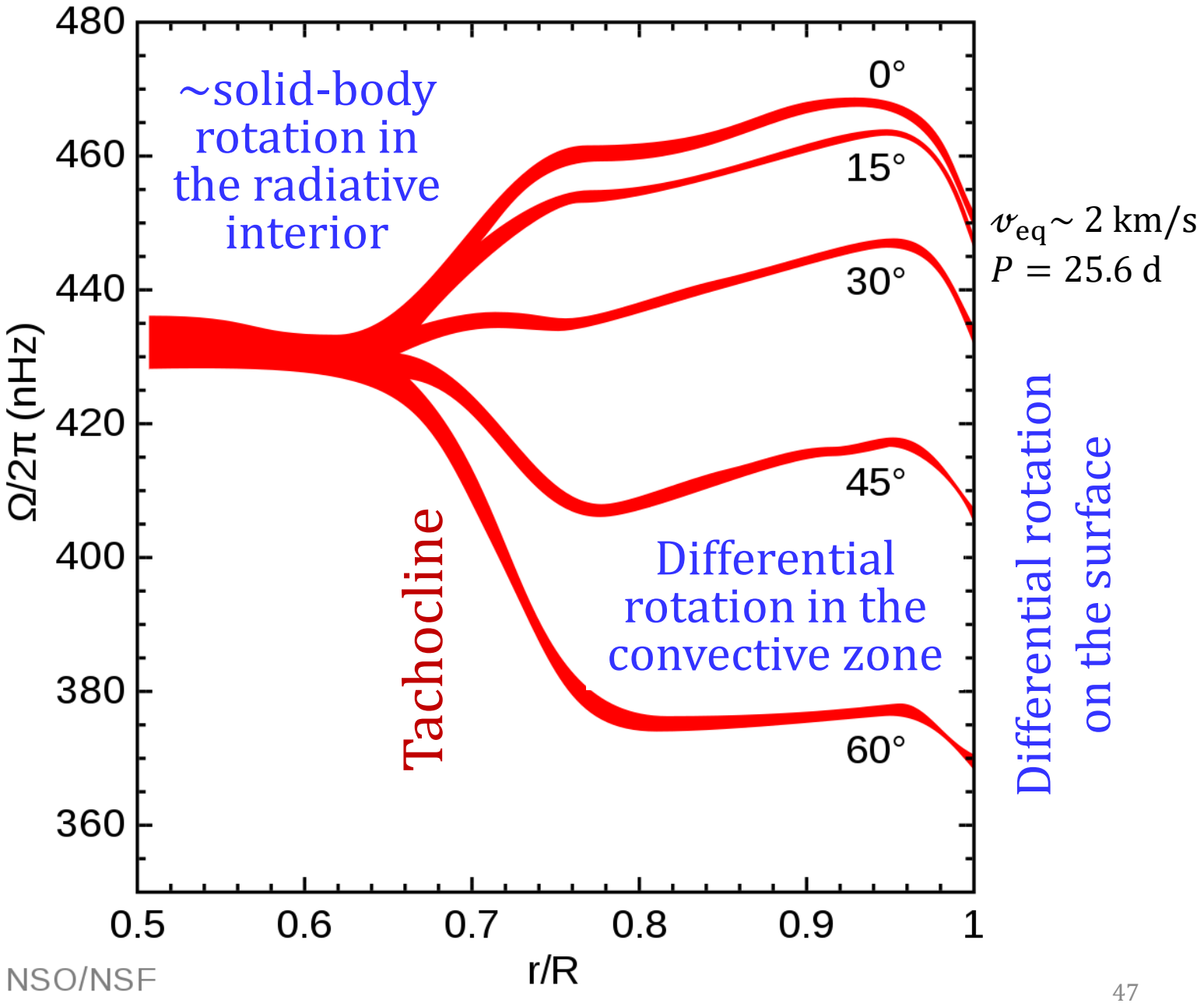

NSO/NSF

Rotation vs Spectral Type

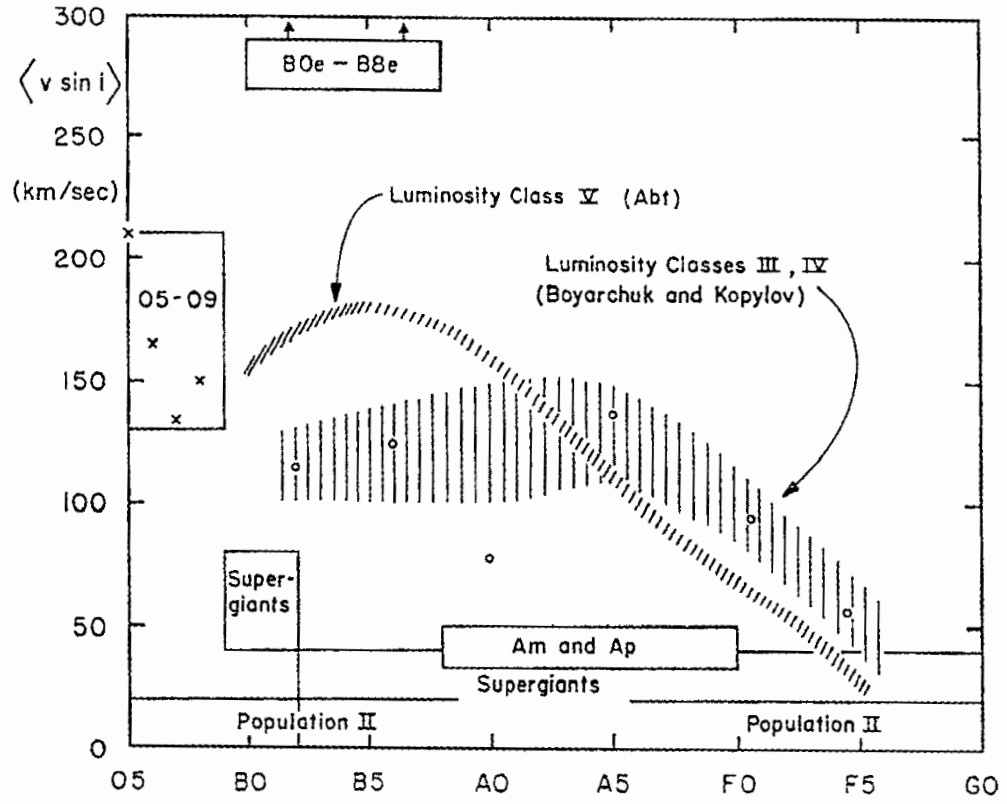

Fig. 3. Projected equatorial velocities, averaged over all possible inclinations, as a function of spectral type. On the main sequence (luminosity class V), early-type stars have rotational velocities that reach and even exceed 200 km/s; these velocities drop to a few km/s for late-type stars, such as the Sun (type G2) (Slettebak [20]; courtesy Gordon & Breach)

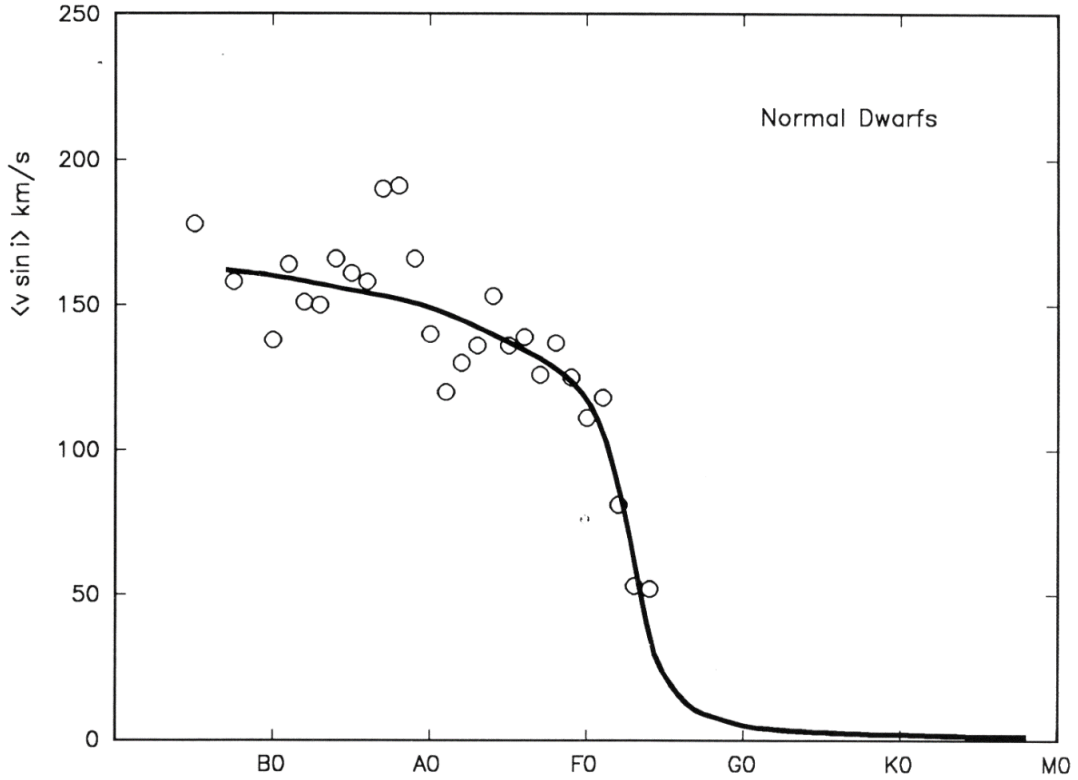

Fig. 17.16. The average rotation rates are shown for spectral intervals as a function of spectral type. (Data are from Uesugi and Fukuda (1982), Soderblom (1983), and Gray (1982b, 1984b).)

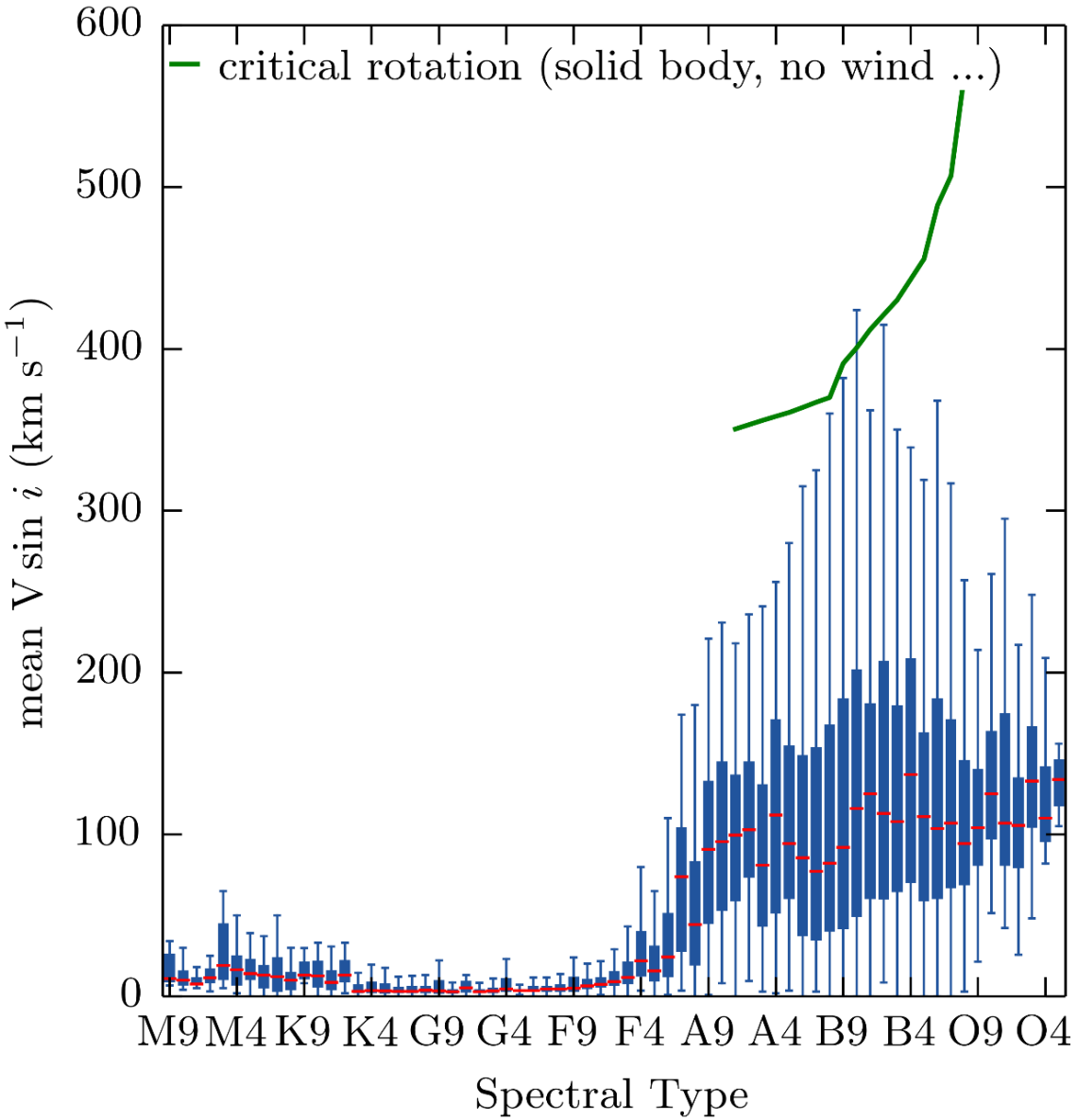

https://aa.oma.be/stellar_rotation

Rotation vs Stellar Mass

- ✓ Massive stars are fast rotators.
- ✓ Rotation declines in the F type (convection? disk?)
- ✓ Low-mass stars spin down quickly early on (disk-star coupling via **B** field), and then experience weak-breaking on the MS due to magnetic breaking and winds.

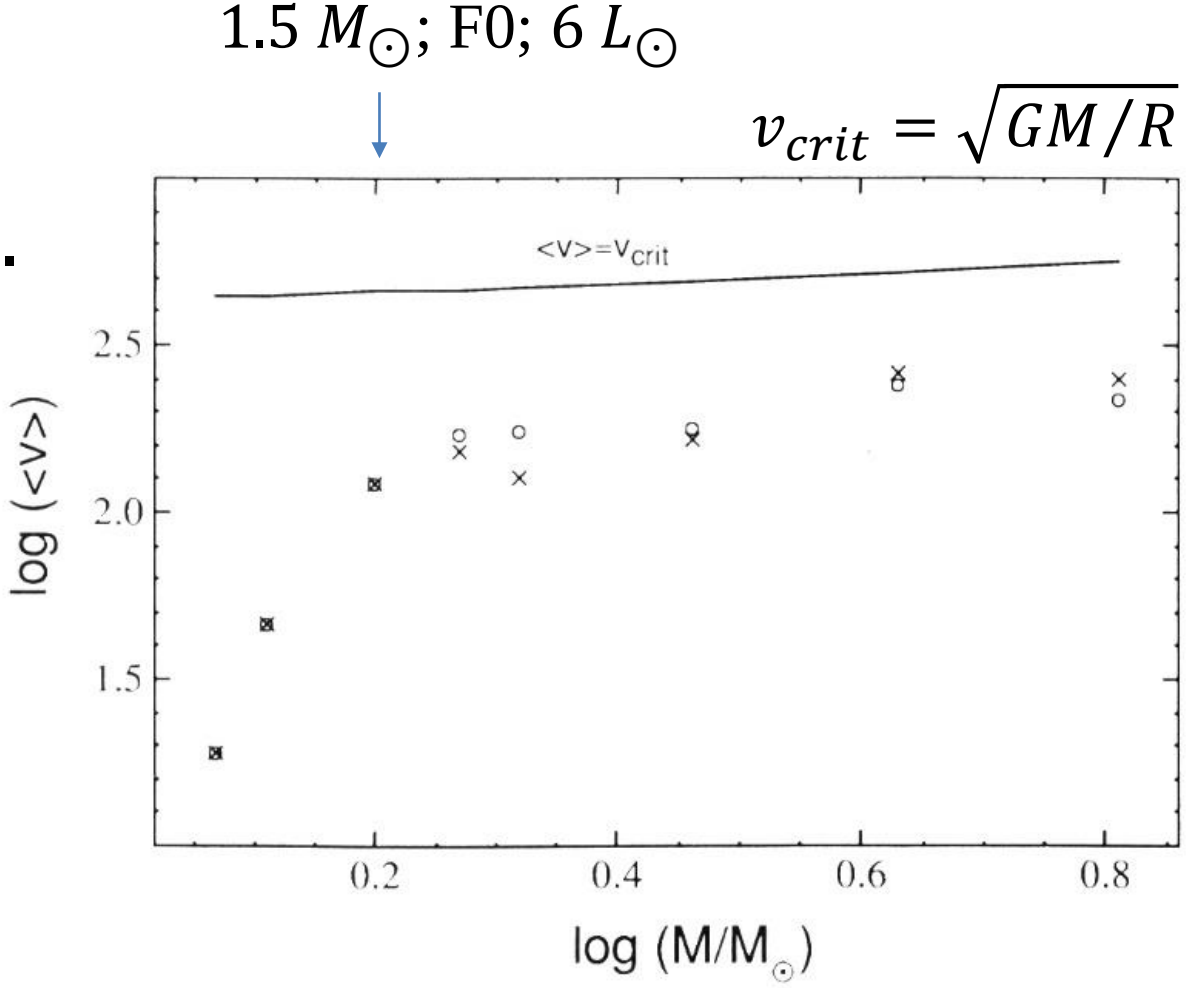

Kawaler (1987)

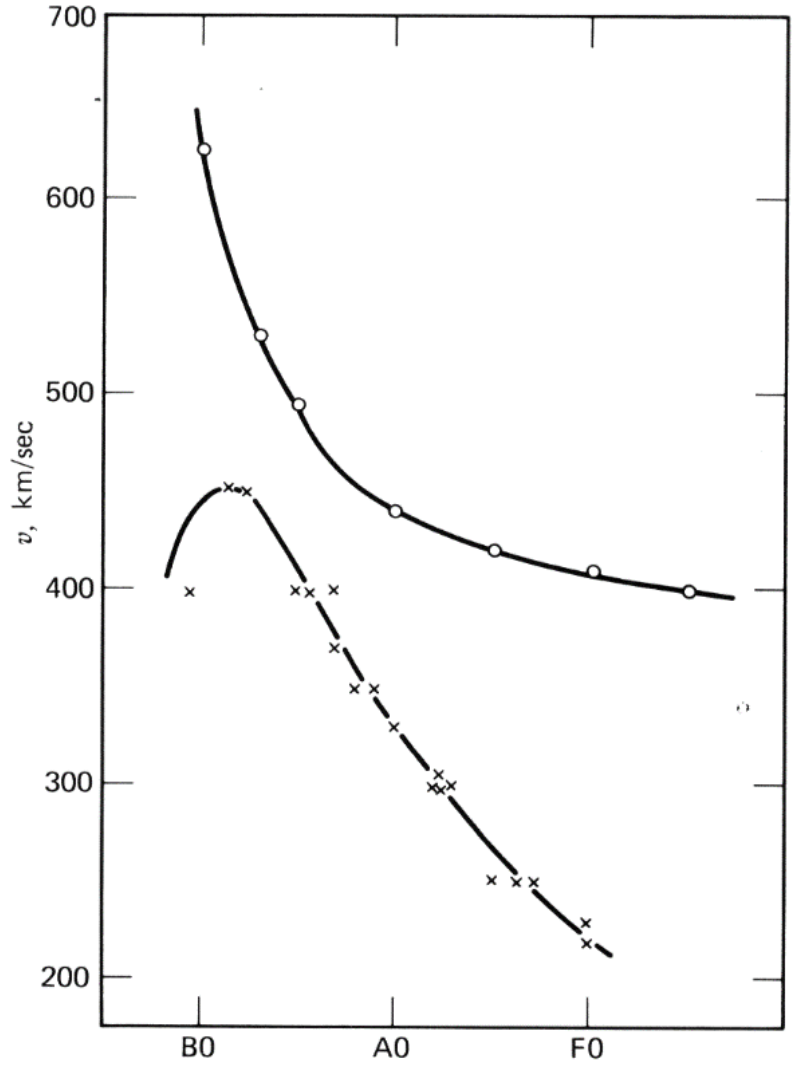

Fig. 17.22. The fastest rotation rates are shown by the × s. The theoretical break-up velocities (top curve) approach the observed relation most closely in the B-star range. (Data from Slettebak (1966).)

- ✓ The fastest <u>single</u> rotators, other than remnant objects such as neutron stars, are Be stars; as fast as ~450 km/s, close to break-up speed
- ✓ Mass loss preferentially along the equators
- ✓ Stars no longer spherical
- ✓ Giants and supergiants rotate slowly because of angular momentum conservation.

Rotation → star cooler and fainter

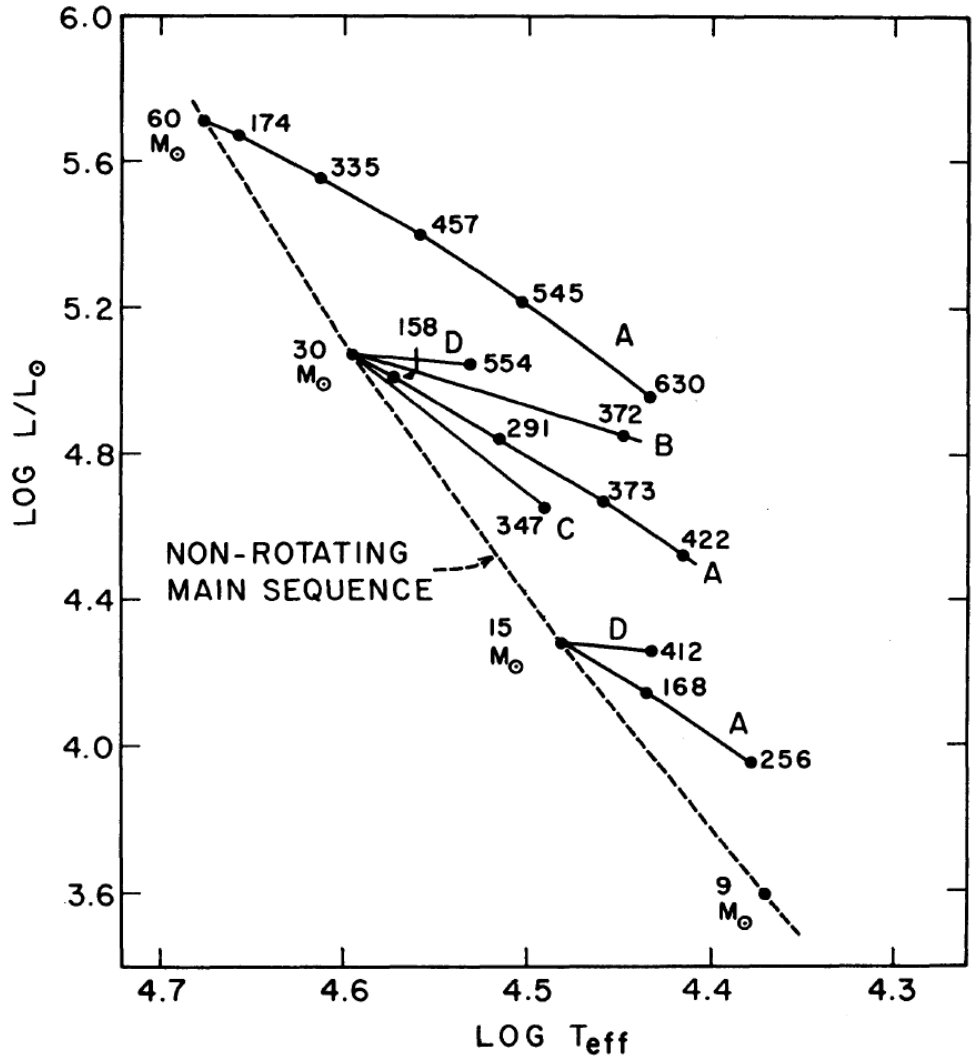

FIG. 2.—Theoretical H-R diagram showing model sequences of increasing angular momentum (*solid curves*). Numbers on curves give calculated velocities at the equator in km sec^{-1}. The distribution of angular momentum for each sequence is indicated by the letter A, B, C, or D.

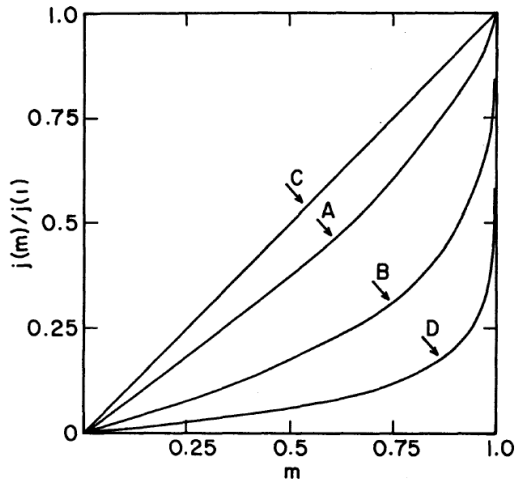

FIG. 1.—Angular momentum per unit mass, as a function of mass fraction interior to a given cylinder about the axis of rotation, for three assumed laws of differential rotation (Cases A, B, and C) and for a uniformly rotating model (Case D) of 30 $\mathfrak{M}_\odot$, log J = 52.73.

D: solid body rotation

Rotation law:
angular momentum distribution $j(m_{\varpi})$ as a function of, m_{ϖ}, the mass fraction interior to the cylinder of radius ϖ about the rotation axis.

Bodenheimer (1971) ApJ, **167**, 153

Rotation
→ line broad and shallow

Line blending

HR 9024 (OU And)
G1 IIIe

HR 3664 G6 III

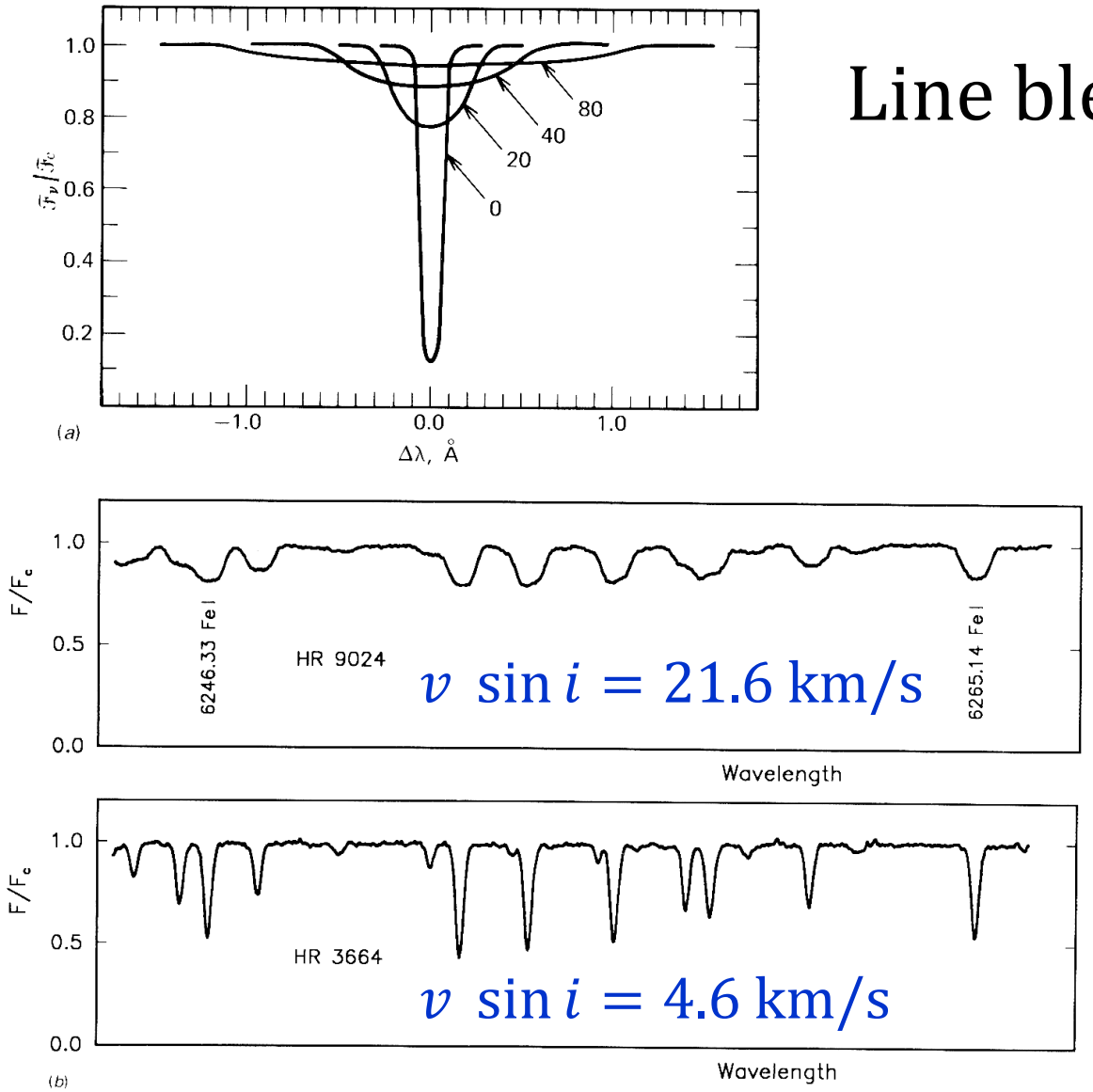

Fig. 17.7. (*a*) Computed profiles illustrate the broadening effect of rotation. The profiles are labeled with $v \sin i$. the wavelength is 4243 Å, and the line has an equivalent width of 100 mÅ. (*b*) These two early-G giants illustrate the Doppler broadening of the line profiles by rotation.

Gray p. 376

Effect of Magnetic Field

Stellar Magnetism

Magnetic field may be important in star formation; governing mass (charged and neutral) flow; ***B*** usually not important in stars, except in compact objects, such as in WDs or NSs.

Typical field strengths

Earth/Sun ~ 1 G
(sunspots ~kG)
Ap/Bp ~10^3 G
White dwarfs ~ 10^6 G
Neutron stars ~ 10^{12} G
Magnetars ~ 10^{15} G (10^{11} teslas)

So stellar magnetism may be important only at the beginning and at the end of a star's life.

Some chemically peculiar (CP) stars, usually hot MS stars (~10%, Ap and Bp stars), with B field in the outer layer to stratify specific elements in the atmospheres (Ap/Bp stars), e.g., He, N, and O to diffuse and settle into deeper layers, while others, e.g., Mn (Manganese 錳), Sr (Strontium 鍶), Y (Yttrium 釔), Zr (Zirconium 鋯) are radially "levitated" to the surface → spectral peculiarities. The bulk chemical composition of the entire star remains normal = that of ISM

Some CP stars have no strong field (Am stars)

THE ASTROPHYSICAL JOURNAL, Vol. 160, May 1970

DIFFUSION PROCESSES IN PECULIAR A STARS

GEORGES MICHAUD*
Hale Observatories, Carnegie Institution of Washington,
California Institute of Technology
Received 1969 September 19

ABSTRACT

It is suggested that diffusion processes are responsible for most of the peculiar abundances observed in Ap stars. If it is assumed that the atmosphere is stable enough for diffusion processes to be important, gravitational settling leads to the underabundances of He, Ne, and O in the stars where they are observed (that is, with the θ_{eff}, log g they are observed to have). Radiation pressure leads to the overabundances of Mn, Sr, Y, Zr, and the rare earths in the stars where they are observed. Silicon would be expected to be overabundant only if it has wide autoionization features. Phosphorus would be expected to be overabundant in stars with $\theta_{eff} \simeq 0.5$, but is observed to be overabundant in stars with $\theta_{eff} \simeq 0.4$.

The magnetic fields observed in Ap stars could bring to the atmosphere the stability needed for diffusion processes to be important. They would also guide diffusion into patches leading to the periodic variation of the observed overabundances.

magnetospheric cavity

accretion columns

accretion hot spots

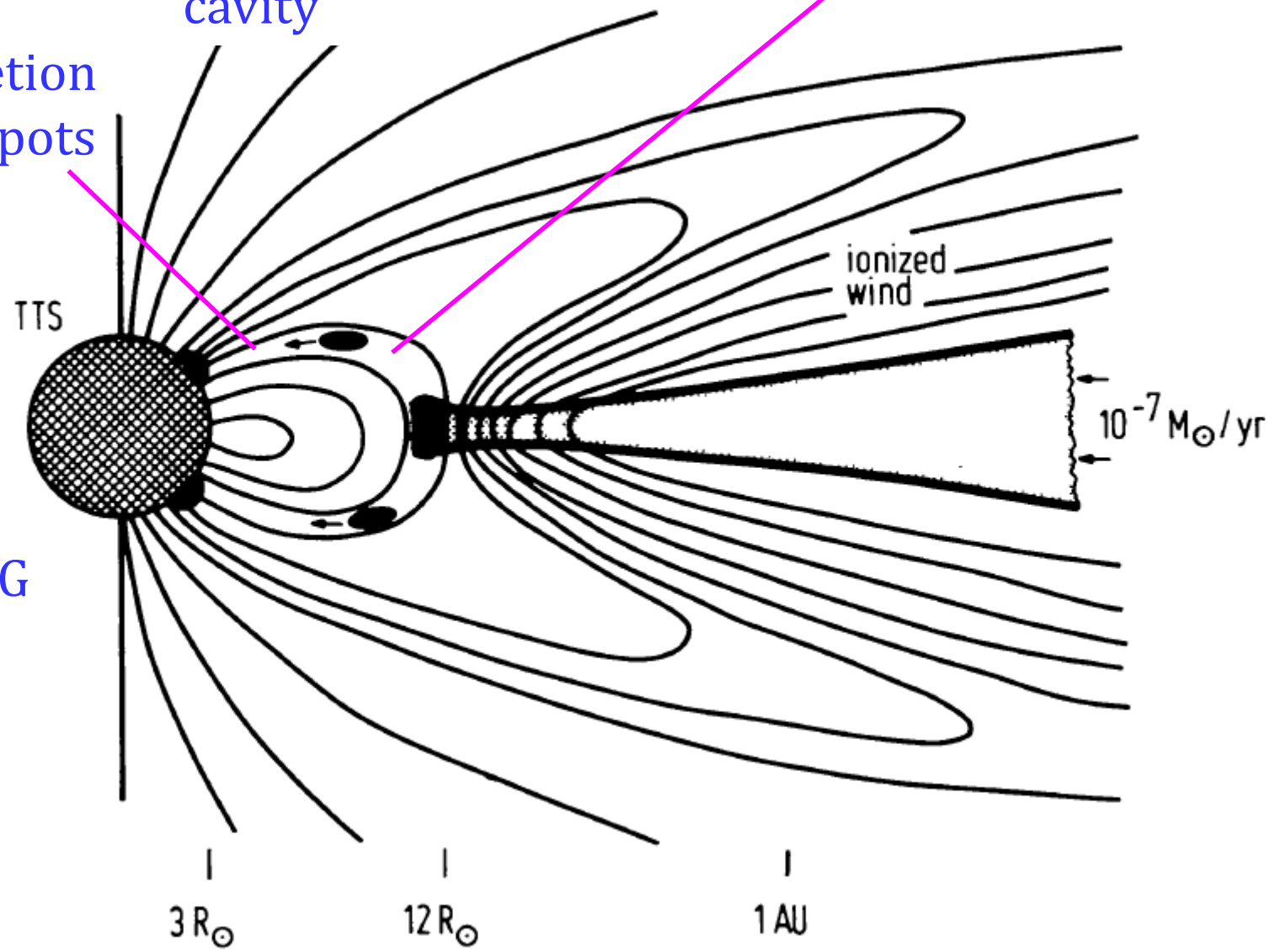

~2 kG

Camenzind 1990

An RS Canum Venaticorum (CVn) binary

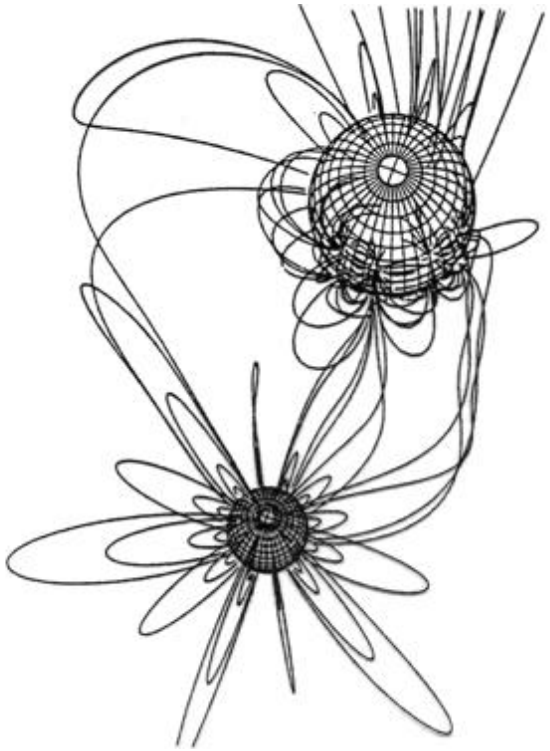

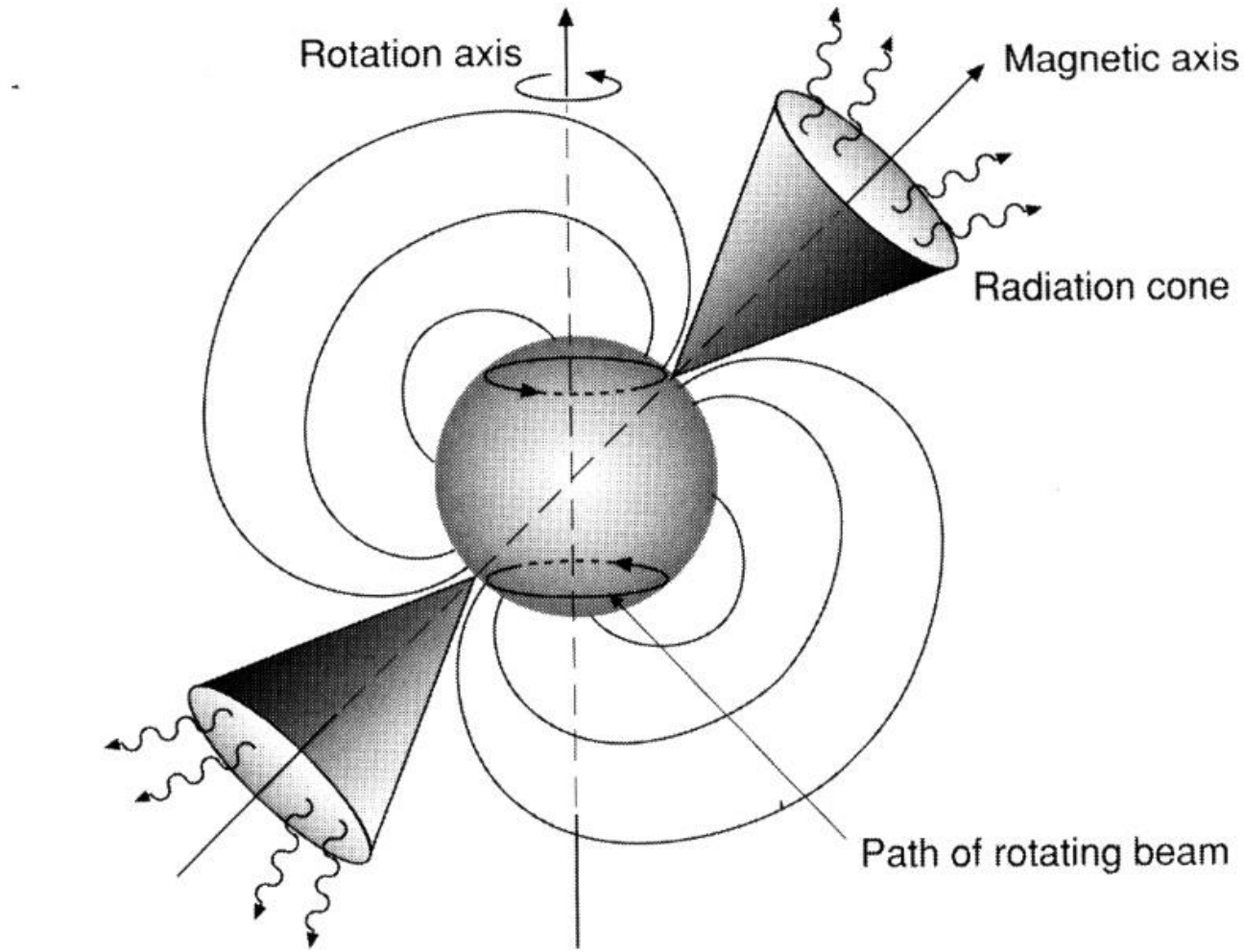

A pulsar is a rapidly rotating neutron star (not pulsating).

If a star has a weak radial magnetic field B_r , and if the star rotates differentially, B_r is stretched horizontally and will be amplified after a few rounds, $\mathrm{B}_\phi \gg B_r$

→ Spruit dynamo

M dwarfs exhibit rapid, irregular flares, bright in the blue and UV.

Ultracool dwarfs (< 1000 K) are magnetized, a few kG, and emit radio radiation

Beginning of an 11-year cycle → a few sunspots appear at mid-latitude; progressively more in number and at lower-latitudes.

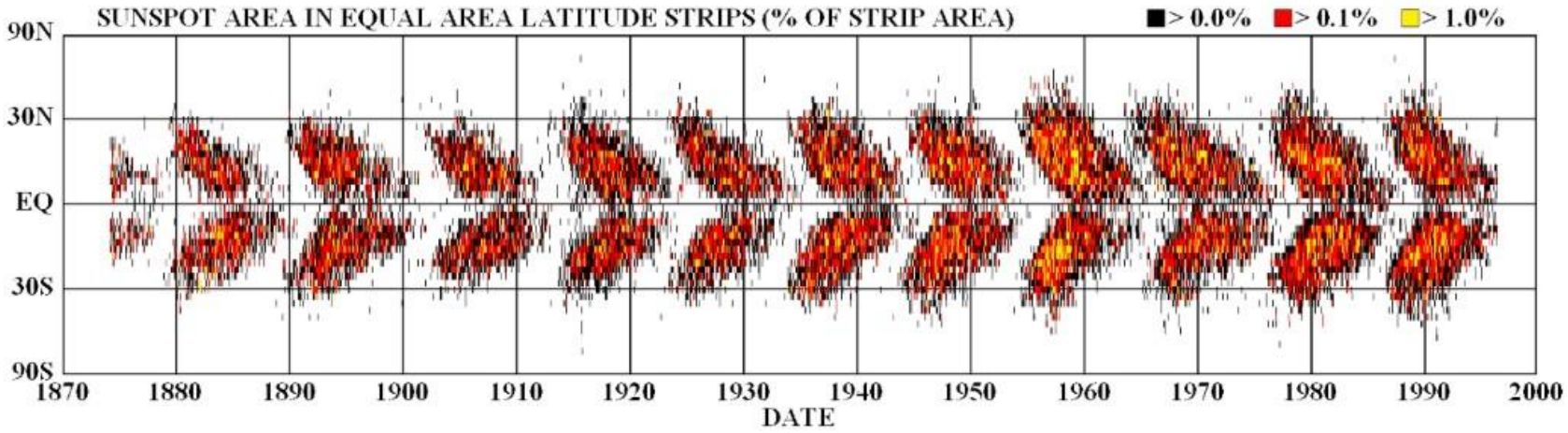

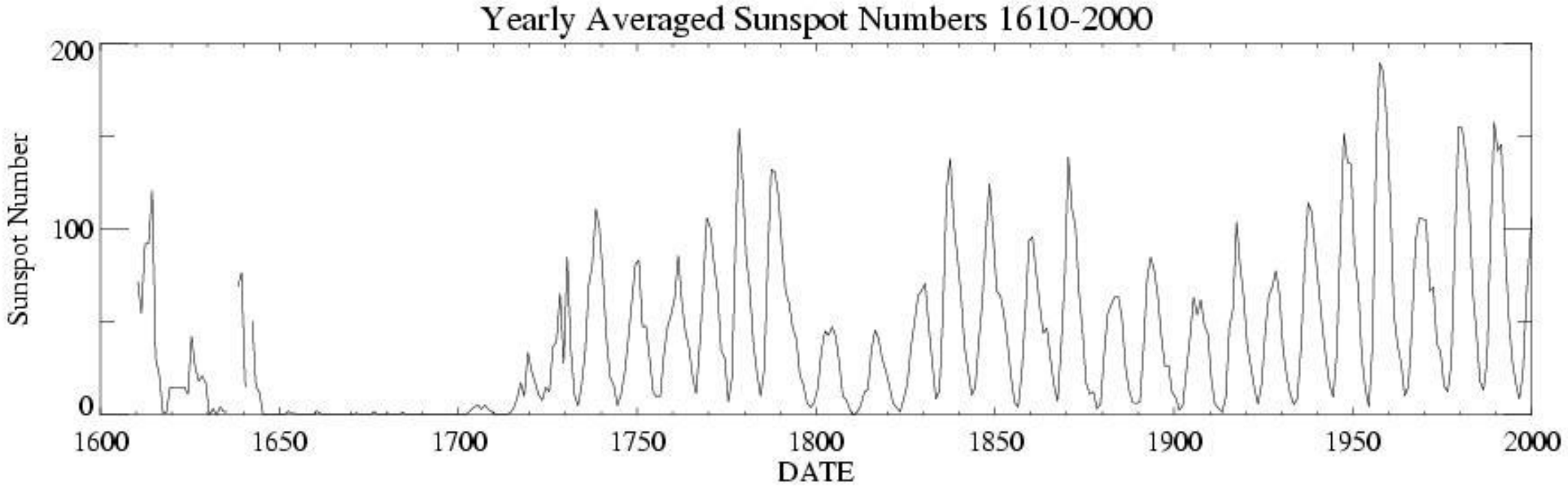

The magnetic field gets increasingly tangled because of the differential rotation. The field breaking through the surface is parallel to the surface and suppresses upward convection → cooler and lower elevation

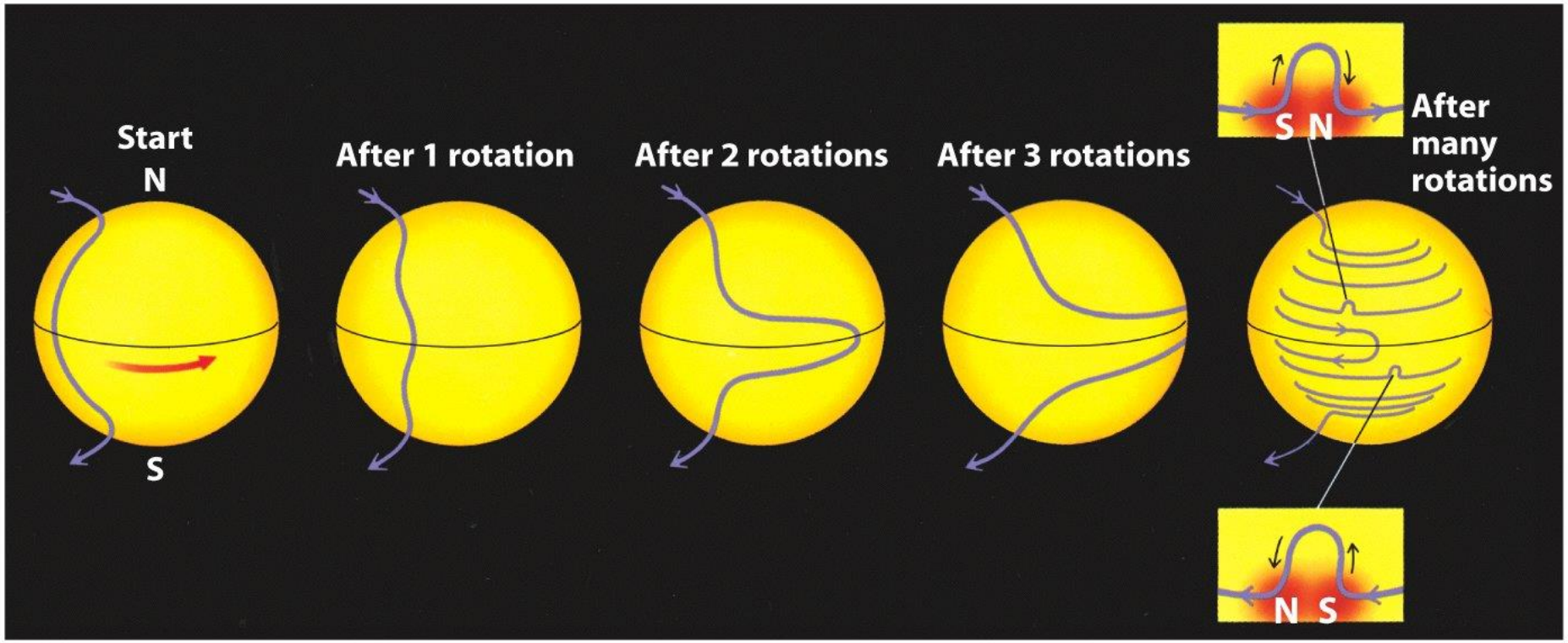

Bobcock's magnetic dynamo model

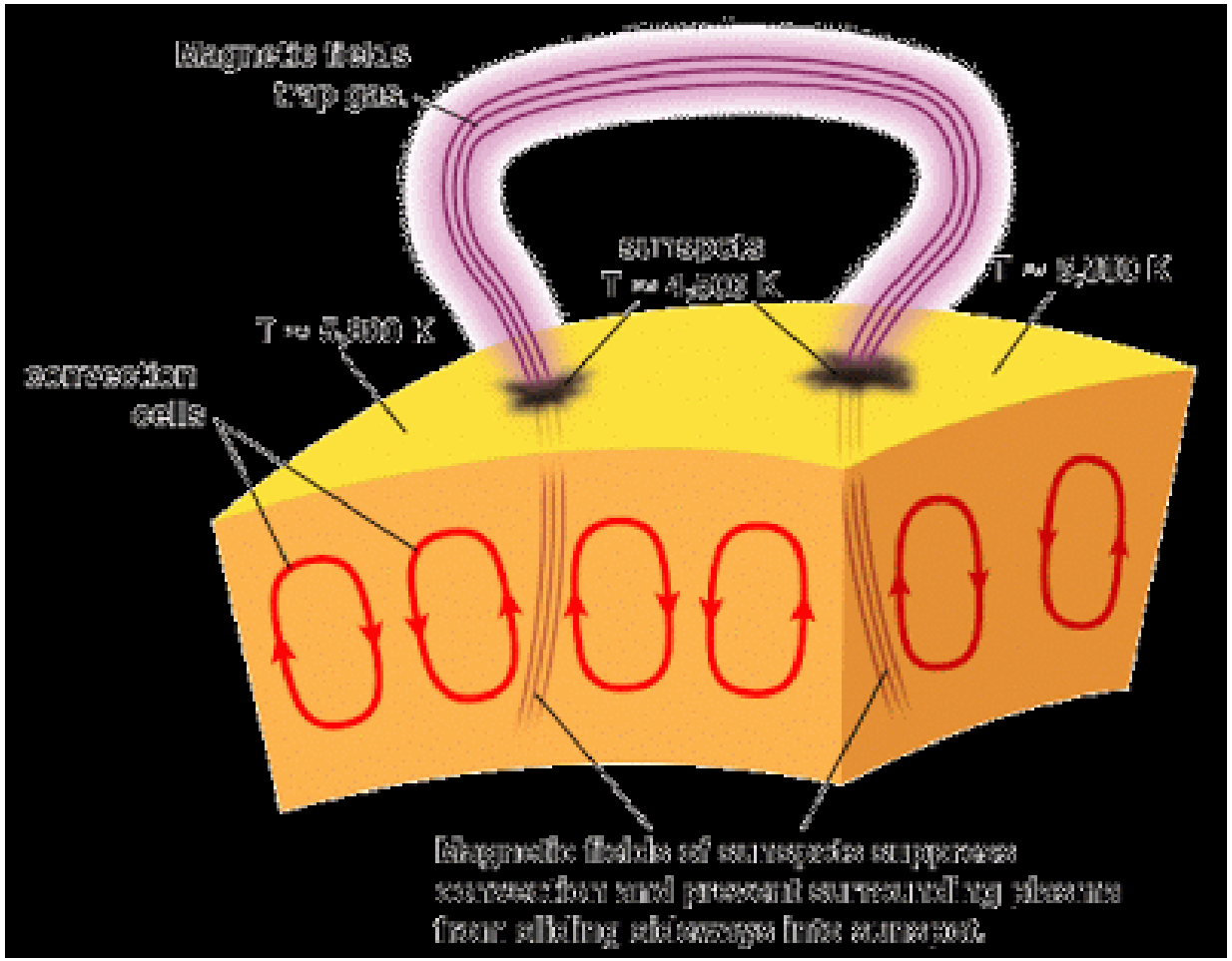
Magnetic field lines trap gas
sunspots
T ≈ 4,000 K
T ≈ 5,000 K
T ≈ 6,000 K
convection cells
Magnetic fields of sunspots suppress convection and prevent surrounding plasma from sliding sideways into sunspot.

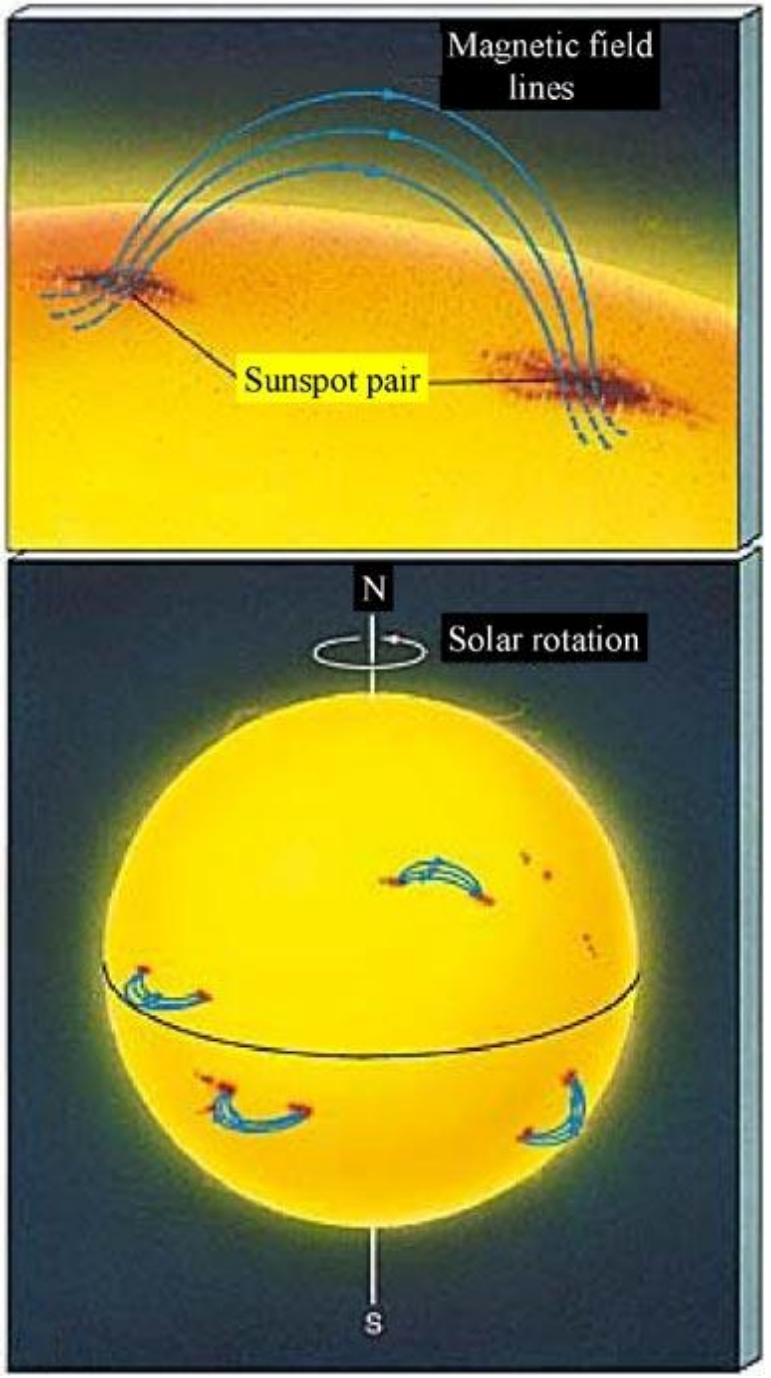
Magnetic field lines
Sunspot pair
N
Solar rotation
S

Surface inhomogeneity (T fluctuations, composition variations, B fields, activity) → distortion across spectral lines as the star rotates

Diagnosed by brightness variations due to starspots, or by **Doppler imaging**

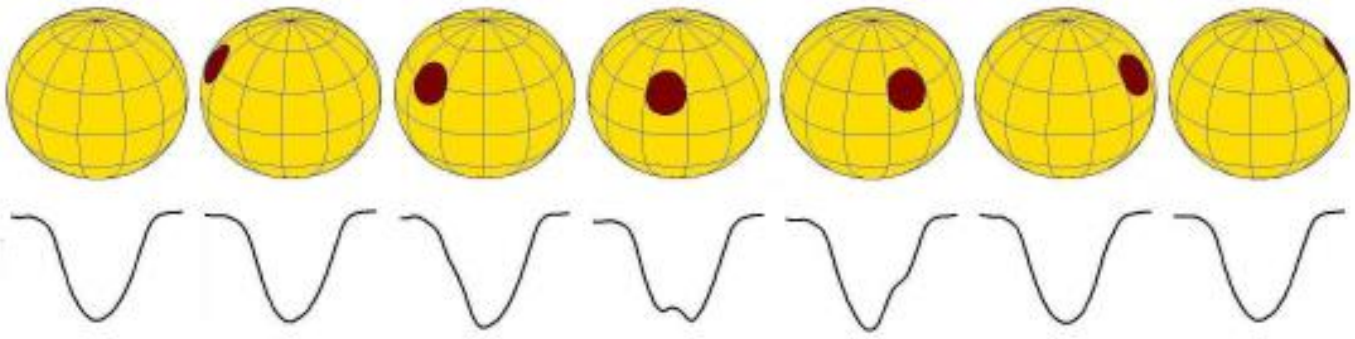

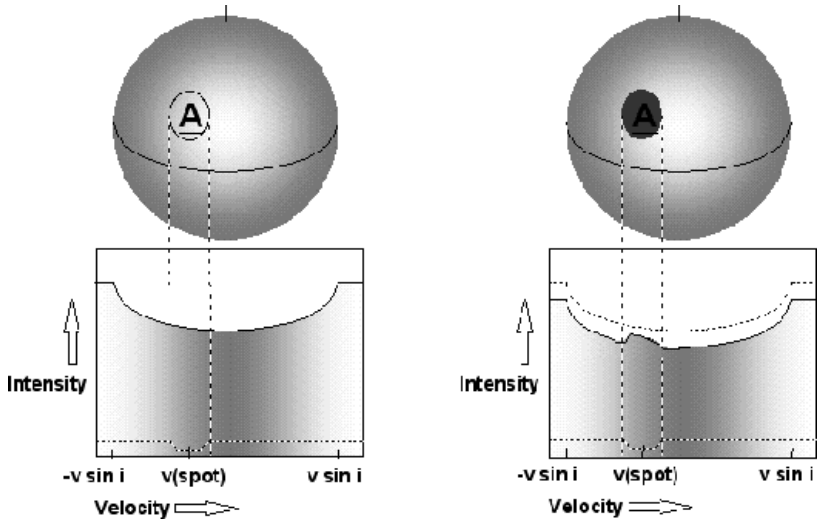

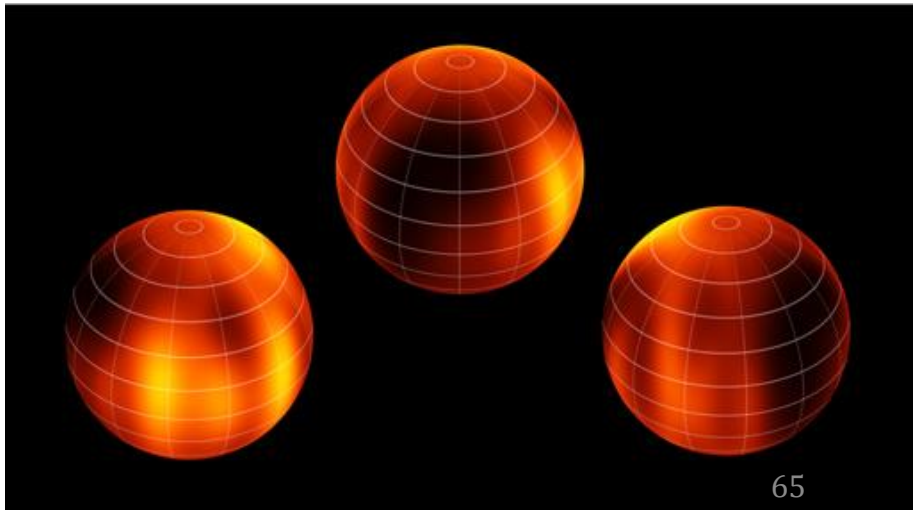

The BD Luhman 16b by the VLT

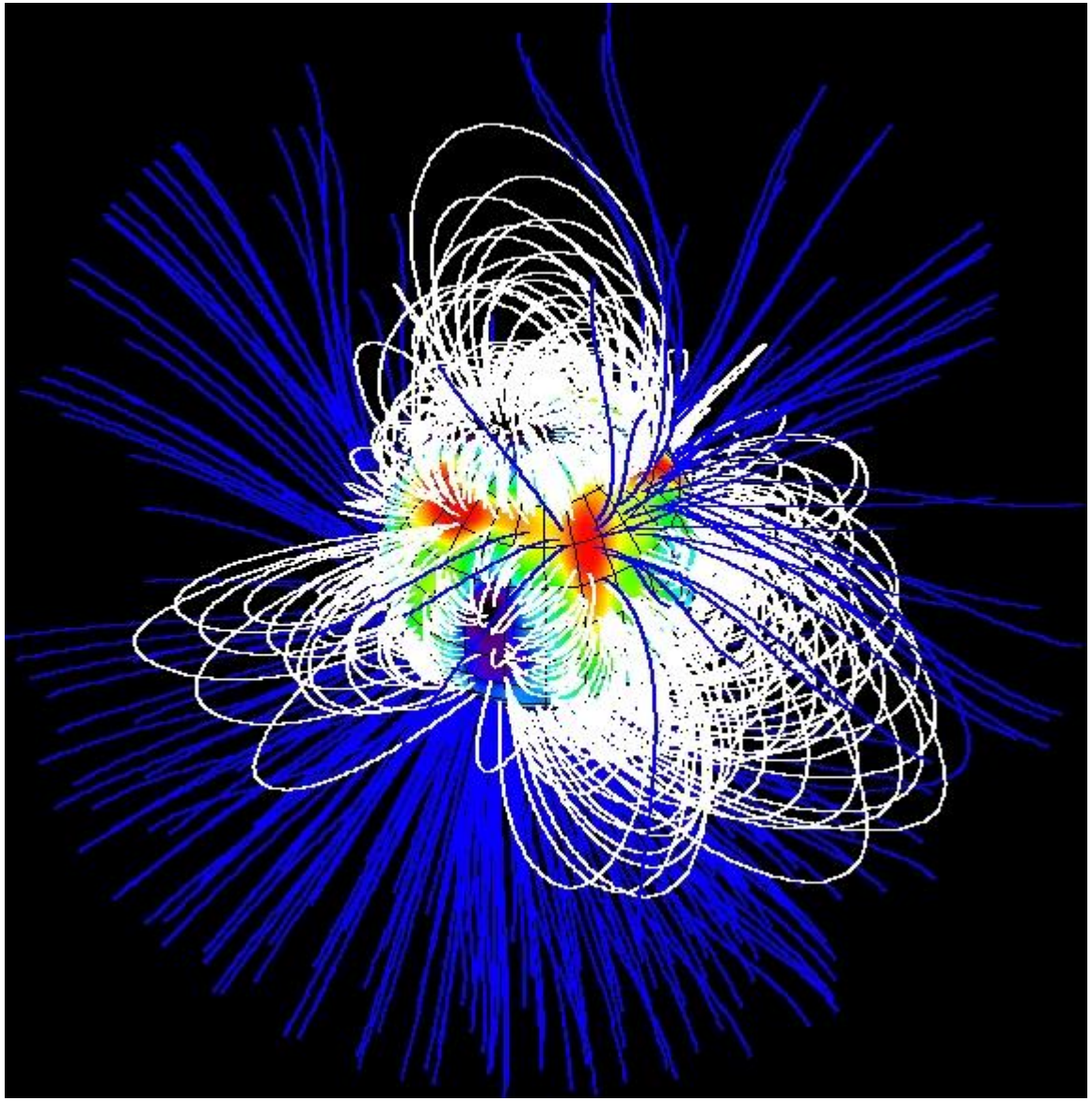

Surface magnetic field of SU Aur (a young star of T Tauri type), reconstructed by means of Zeeman-Doppler imaging

Effect of Binarity

Binary Stars

The binary fraction of young stars comparable to that of MS stars.

Star formation = Binary formation = Cluster formation

One of the solutions (alternative: a disk and planets) to the angular momentum problem during SF

Intricate magnetic interaction between binary components

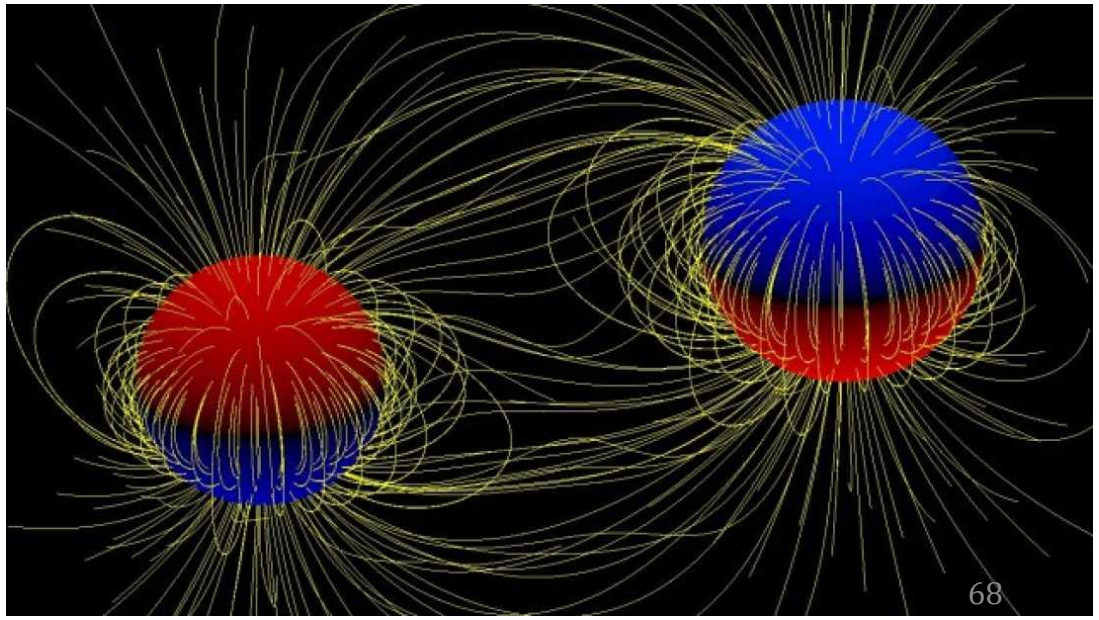

Solar-type stars,
(singles):(doubles):(triples):(quadrupoles)=42:46:9:2
(Abt & Levy 1976)

A smooth period distribution peaking ~14 yrs

Mass ratio → fission (for close pairs), and separate protostellar contraction (for wide pairs)

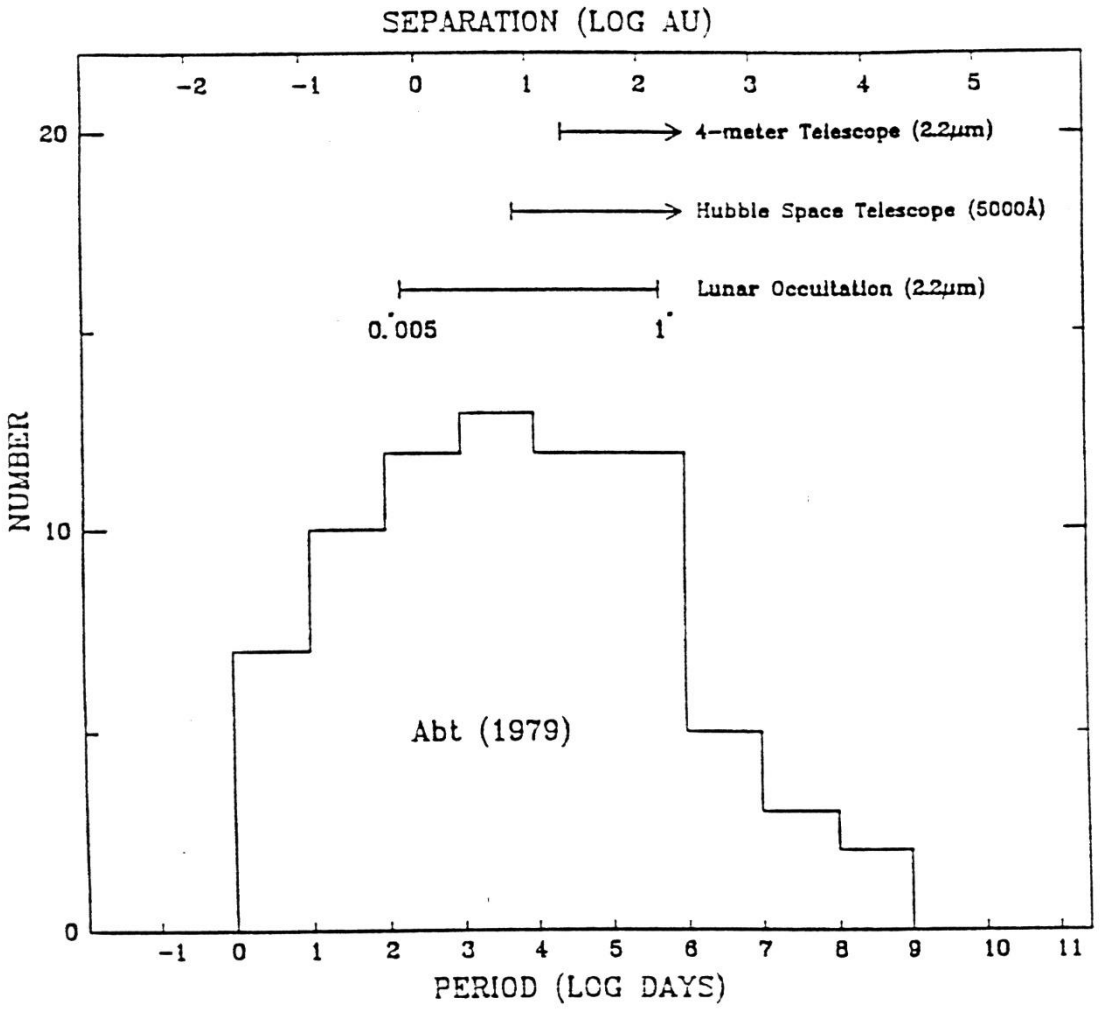

Close binaries → mass and momentum exchanges

Originally more massive component as the primary

Strong tidal forces → orbit/spin synchronization

Detached; semi-detached; contact systems

Some with common envelopes

Numerous high-energy phenomena

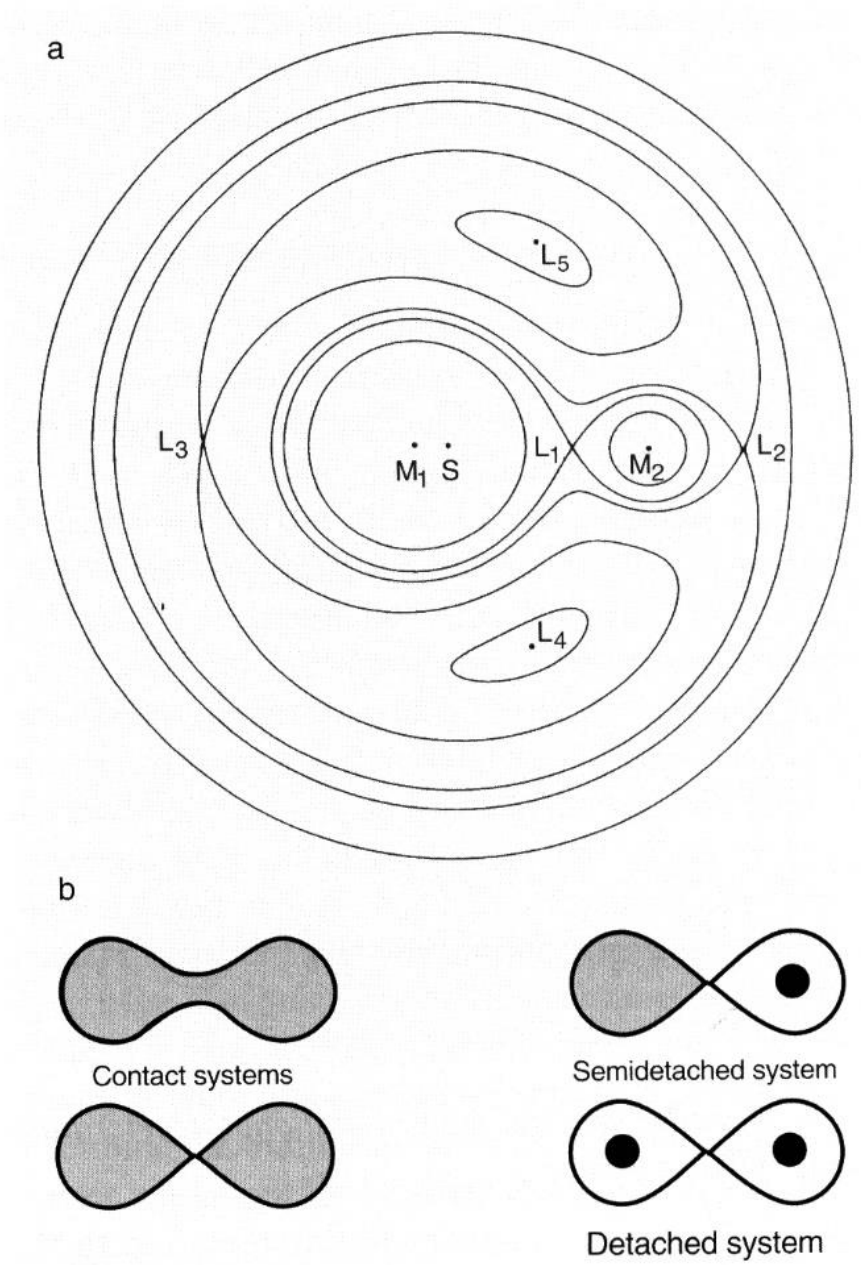

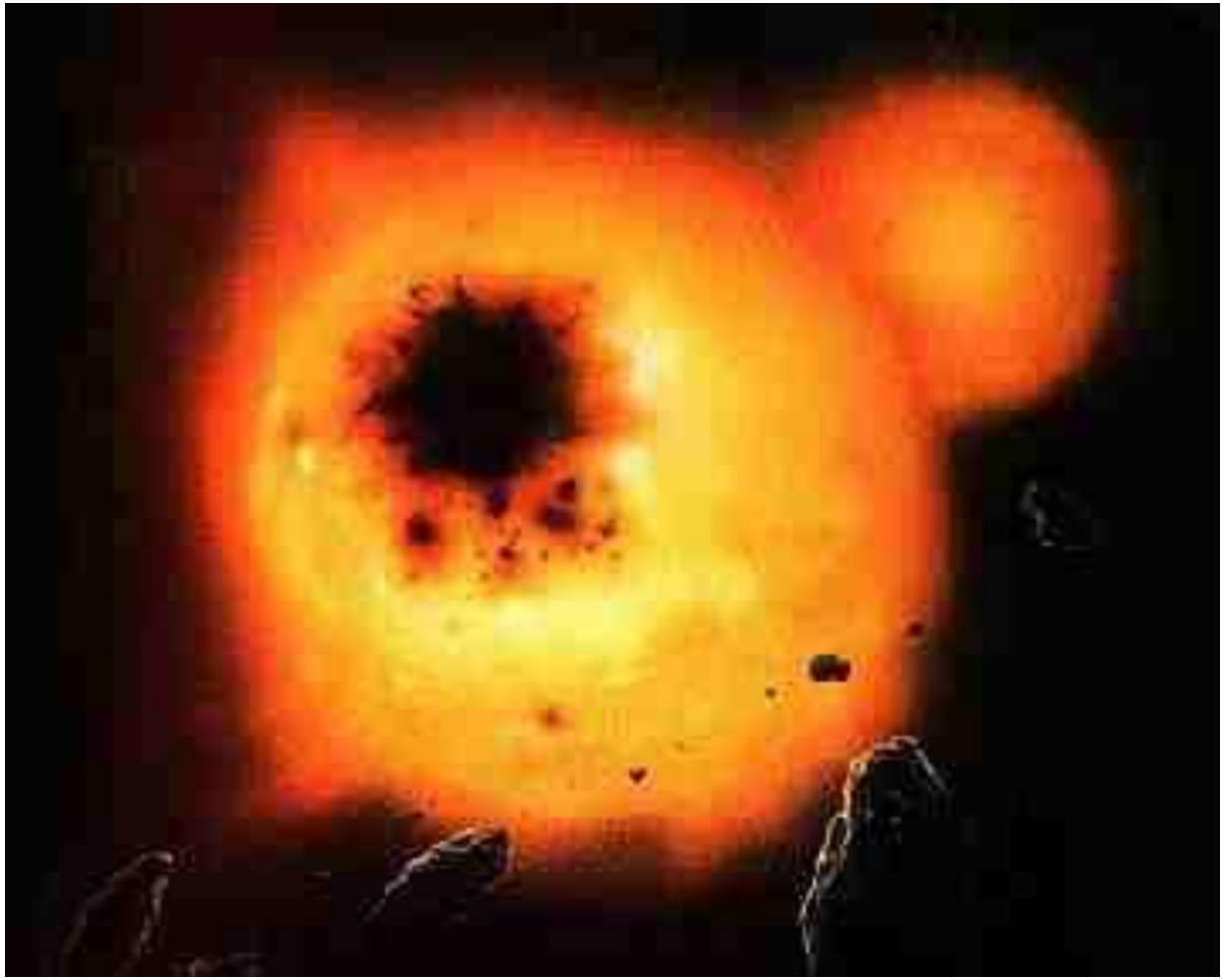

RS CVn stars: eruptive variables and close binary systems

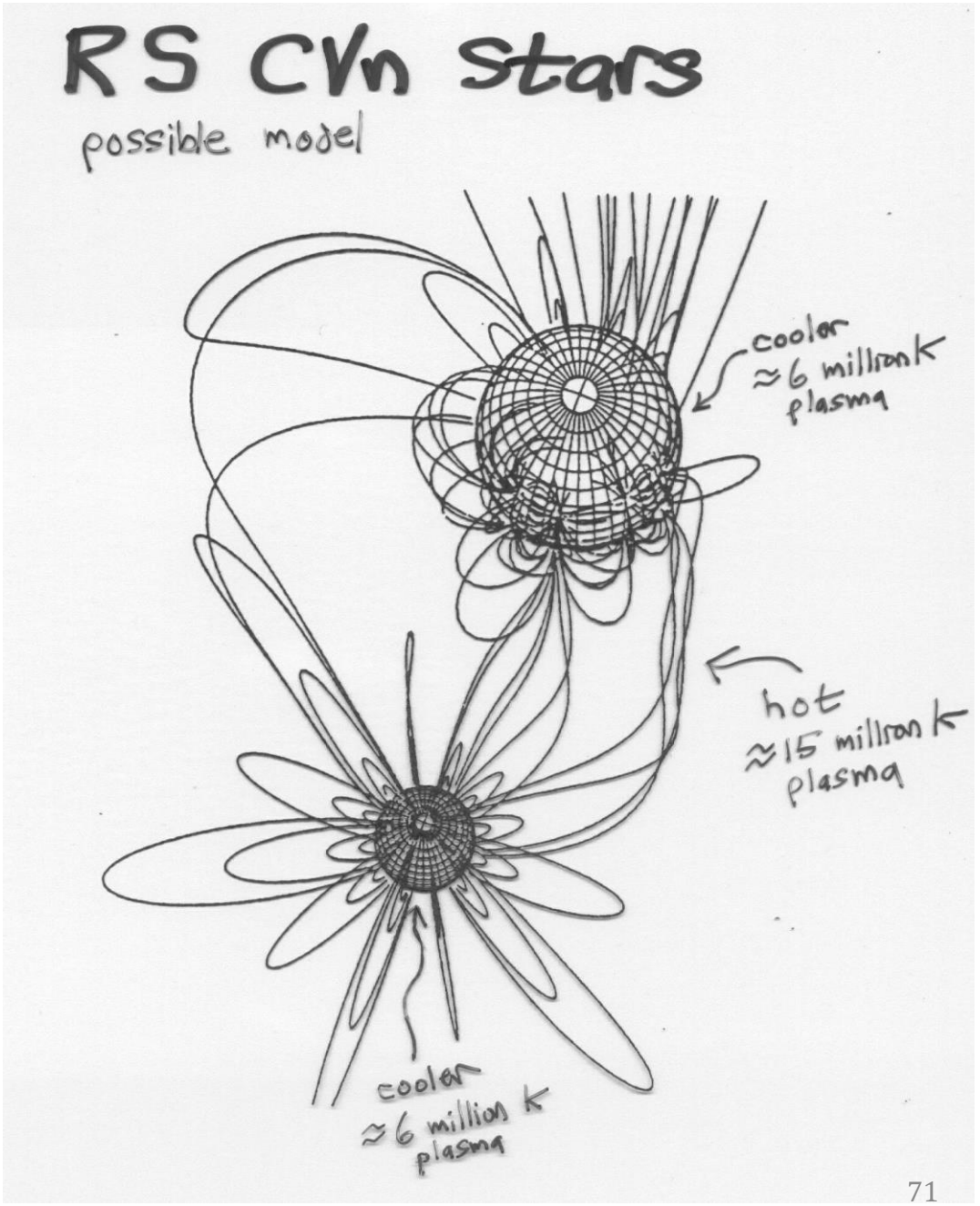

Effect of Mass Loss

Mass Loss

Every star loses mass in every stage of evolution.

$$\frac{1}{2}mv_{esc}^2 = \frac{GMm}{R}$$

i.e., due to kinetic energy of gas at the stellar surface.

Alternatively, there could be mechanisms to accelerate the particles, e.g., coronal winds (stars with surface convection → acoustic waves, like the Sun), radiative winds (photon momentum), line-driven (continuum-driven, dust-driven) winds, rotation-driven (pulsation-driven) winds.

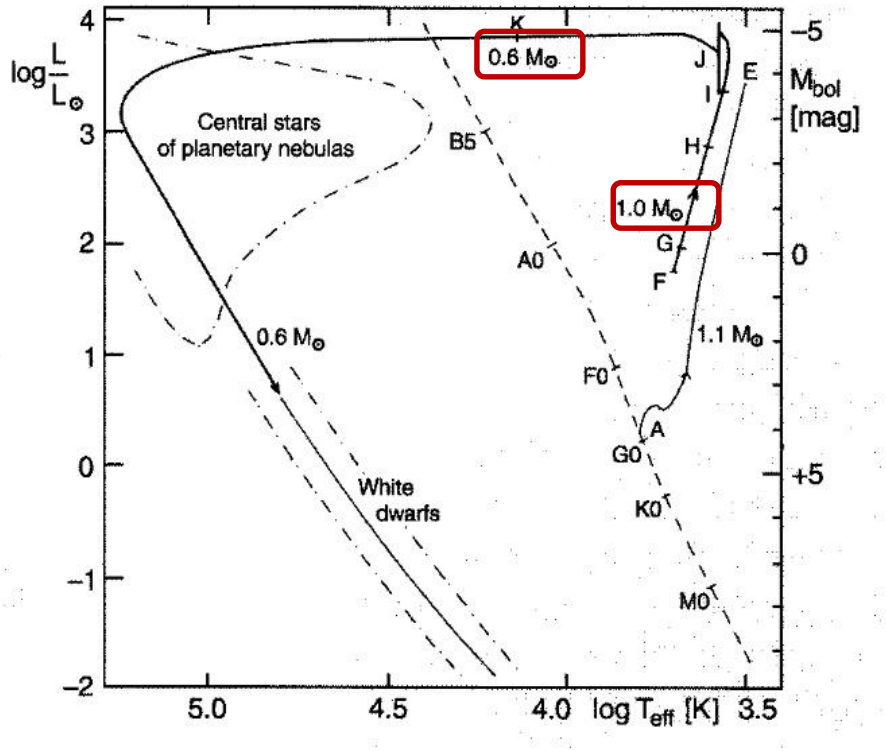

Fig. 8.8. The evolutionary paths in the Hertzsprung–Russell diagram of Population I stars having 1.0 $\mathcal{M}_\odot$ and 1.1 $\mathcal{M}_\odot$, from central hydrogen burning (A) to the helium flash (E), without taking mass losses into account. After A. V. Sweigart and P. G. Gross (1978). The ejection of a mass of 0.1 $\mathcal{M}_\odot$ during the helium flash was assumed. The further evolution of the star of 1.0 $\mathcal{M}_\odot$ was calculated taking the mass loss according to (7.105) into account, after D. Schönberner (1979). F → G: the asymptotic giant branch; only one of the thermal pulses (helium flashes) which occur after I is drawn in, at J. The mass loss becomes important at H and leads to a final mass of 0.6 $\mathcal{M}_\odot$, which is reached at K

Mass loss (Reimers 1975)

$$\dot{M} \approx 4 \times 10^{-13} \frac{L/L_\odot}{(g/g_\odot)\ (R/R_\odot)} \ [\mathrm{M_\odot\ yr^{-1}}]$$

$$g = GM/R^2$$

Sun now $\dot{M} \approx 2 \times 10^{-14}\ \mathrm{M_\odot\ yr^{-1}}$

Cool supergiant $\dot{M} \approx 10^{-7}$ to $10^{-5}\ \mathrm{M_\odot\ yr^{-1}}$

Unsöld

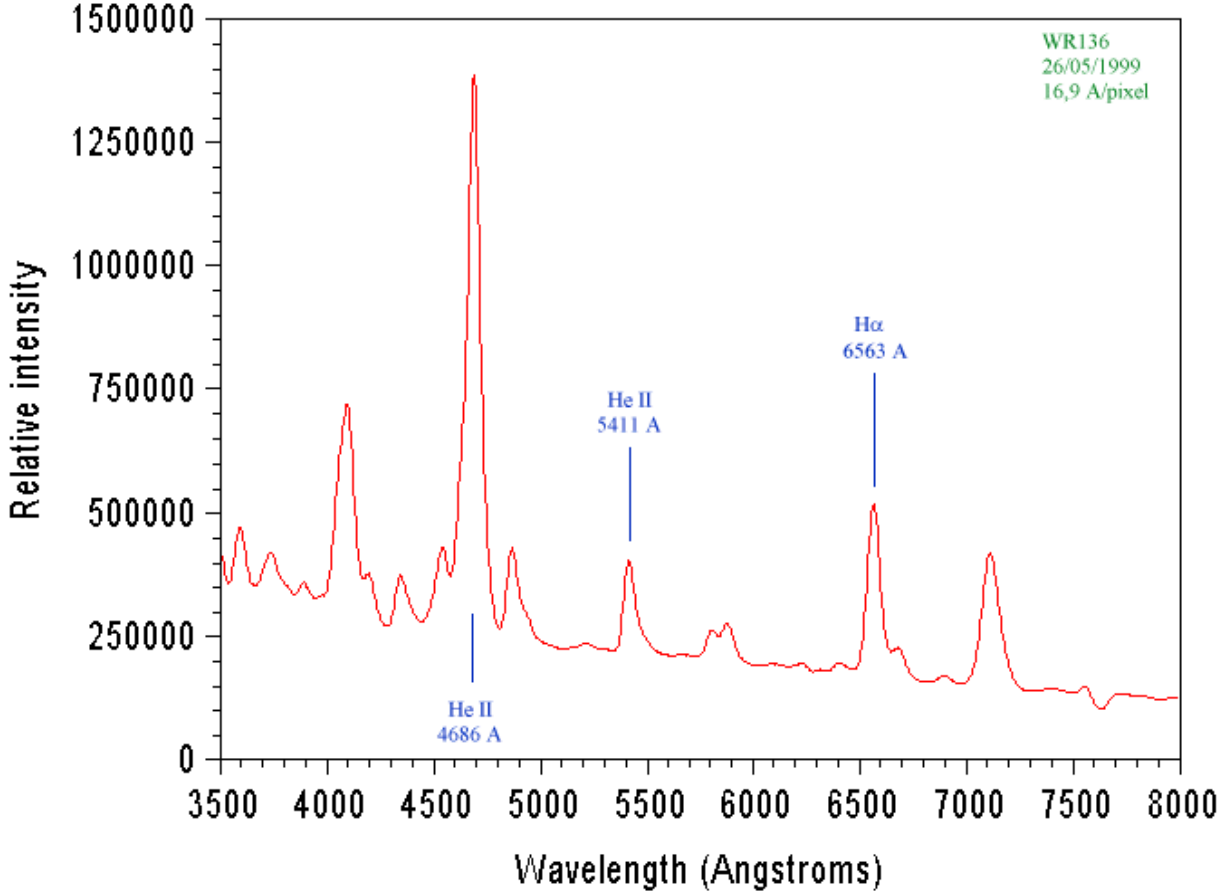

WR stars

$T_{eff} \sim 25{,}000$ to $50{,}000$ K

Evolved massive ($\gtrsim 20 M_\odot$) stars

Wind $\sim 2000\ km\ s^{-1}$

$\dot{m} \sim 10^{-5} M_\odot\ yr^{-1}$

Spectrum of a Wolf-Rayet star

$O (\rightarrow WN) \rightarrow LBV \rightarrow \begin{matrix} WN \\ WC \end{matrix}$

$\rightarrow SNIb,c$

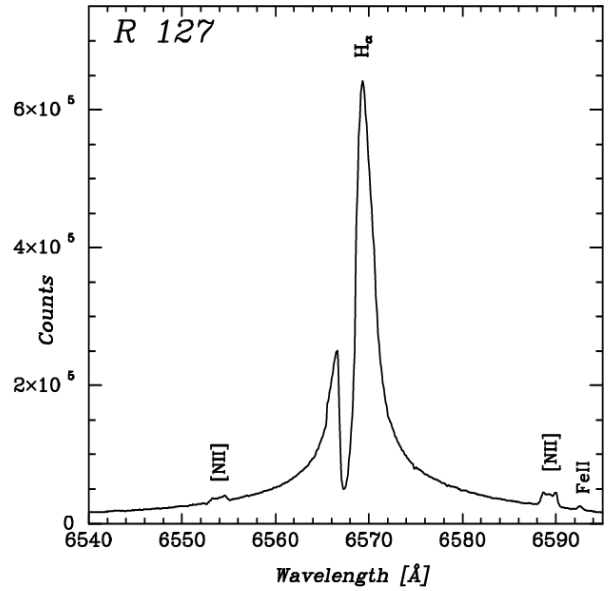

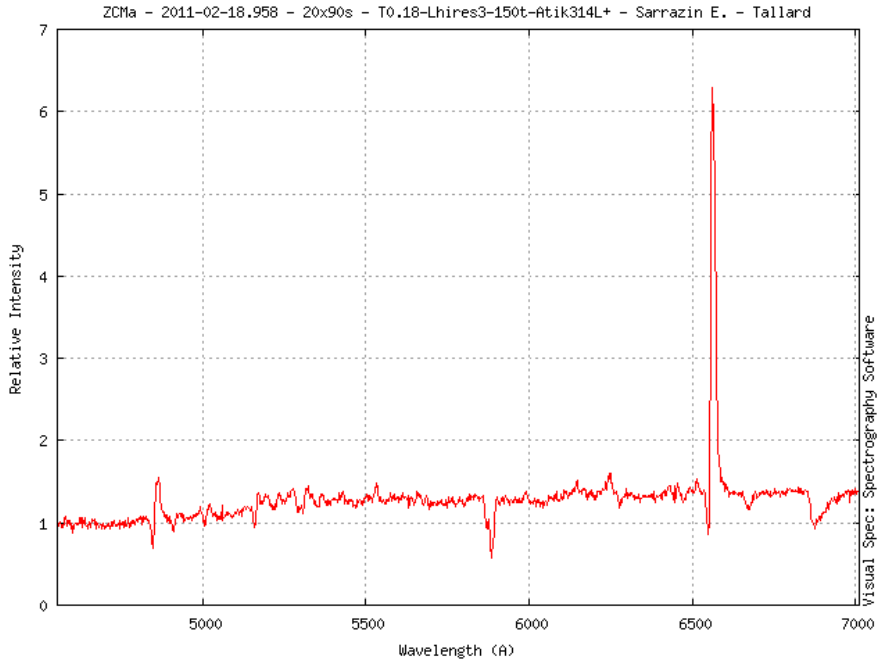

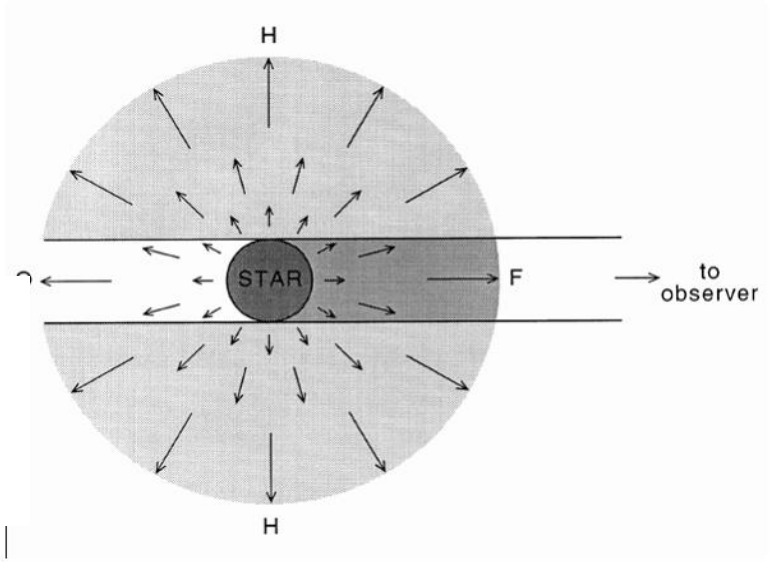

P Cygni profile of a spectral line --- a blue-shifted absorption superimposed on an emission line → **mass loss** (cool gas toward us)

Lamers and Cassinelli, *Introduction to Stellar Winds*, Cambridge, 1999

Stellar Variability

Every star varies in brightness.

The solar constant

The flux density of the solar irradiance at 1 au, including all frequencies

It is an average value; the solar constant is not a physical constant; varies

1.361 kW/m^2 at solar minimum; 0.1% greater at solar maximum

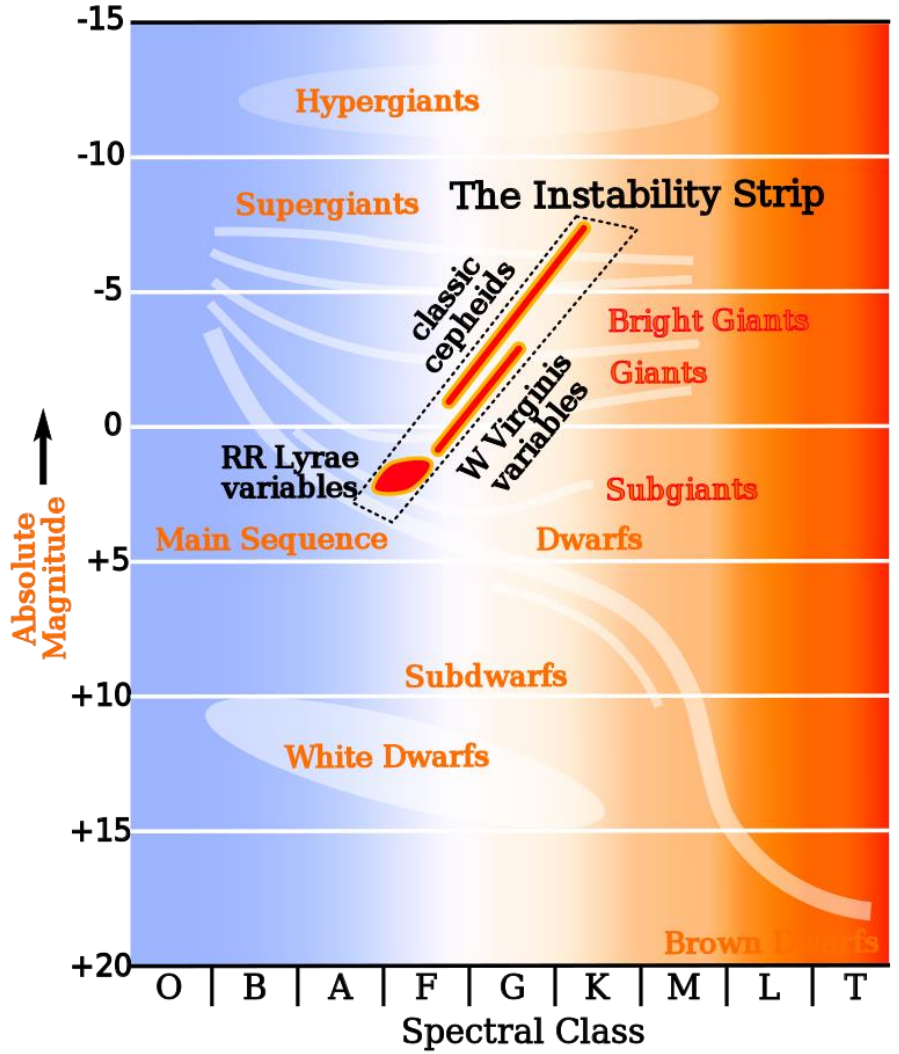

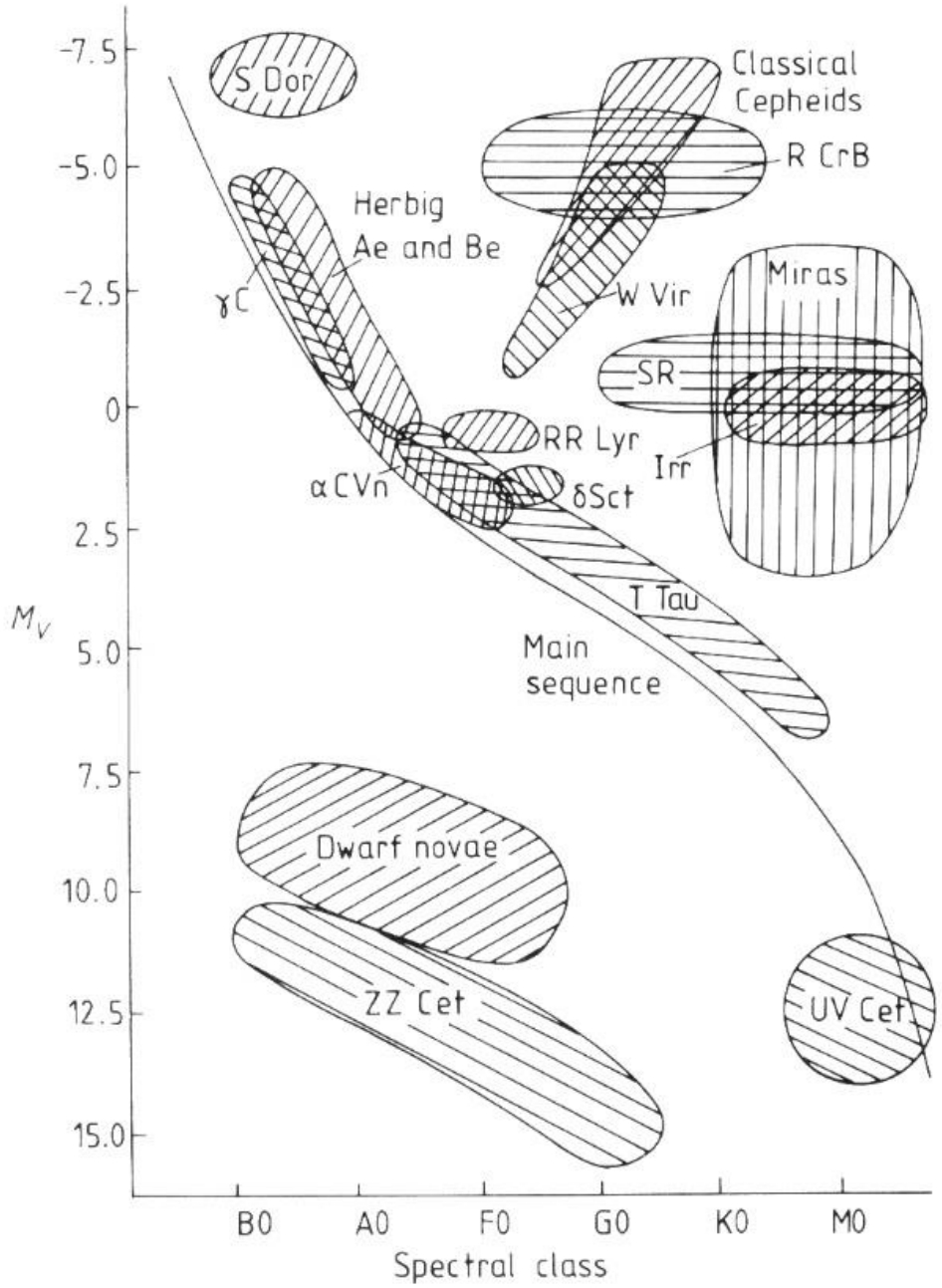
-7.5
-5.0
-2.5
0
2.5
5.0
7.5
10.0
12.5
15.0
M_V
S Dor
Classical
Cepheids
R CrB
Herbig
Ae and Be
γC
W Vir
Miras
SR
RR Lyr
Irr
αCVn
δSct
T Tau
Main
sequence
Dwarf novae
ZZ Cet
UV Cet
B0
A0
F0
G0
K0
M0
Spectral class

Kitchin

Intrinsic variability *physical*

- ✓ Pulsating (RR Lyr; Cepheids, RV Tau; Mira; δ Scu; ZZ Ceti)
- ✓ Rotational (magnetic, spotted)
- ✓ Eruptive (novae, SNe, CVs, X-ray binaries; symbiotic; flare)

Extrinsic variability *non-physical*

- ✓ Eclipsing (by stars, planets, dust clumps; EA; EB; EW)
- ✓ Gravitational microlensing

Some young variability (Orion var., T Tauri stars, Be stars) could have more than one mechanism.

Period-luminosity relation for pulsating variables

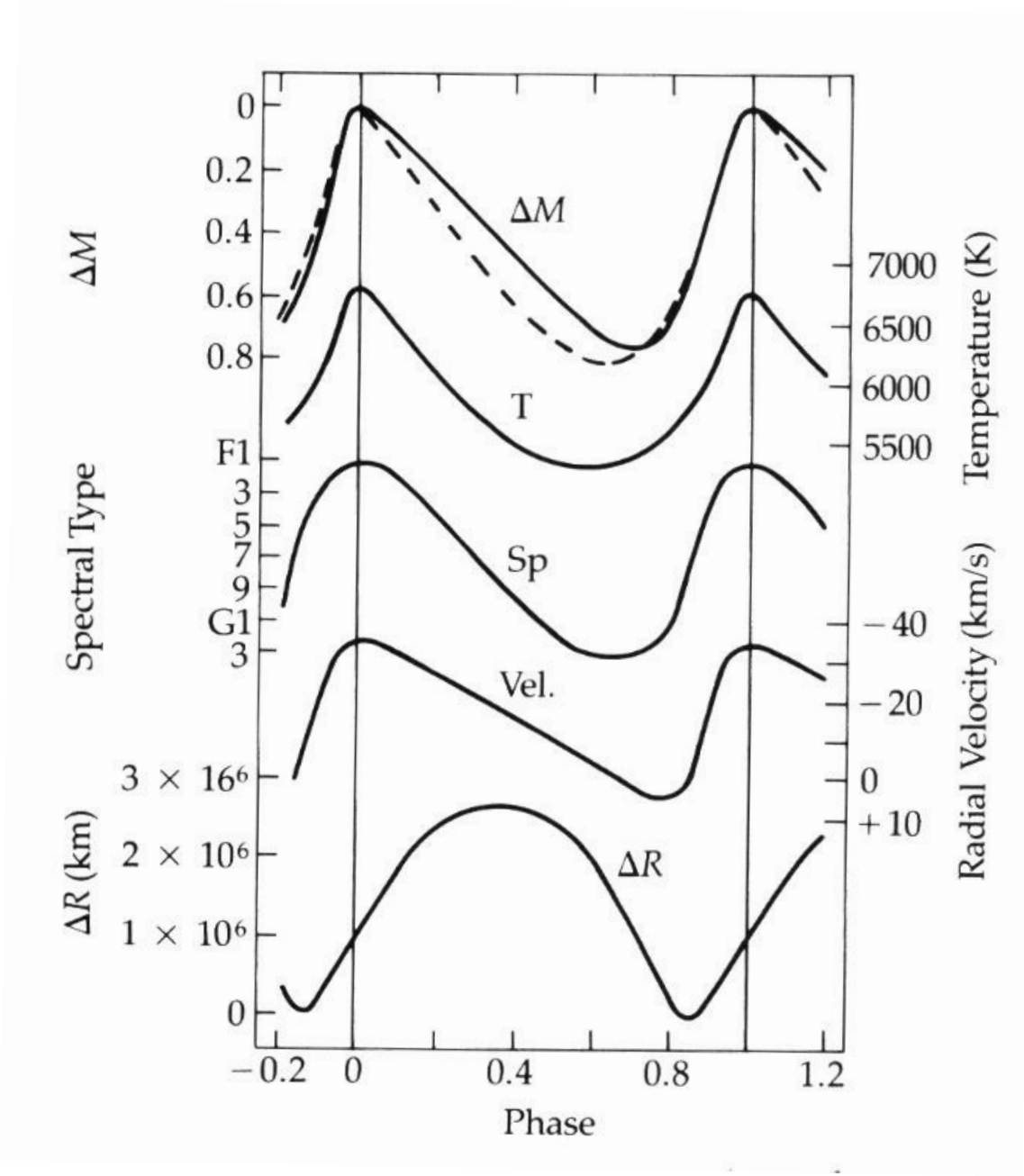

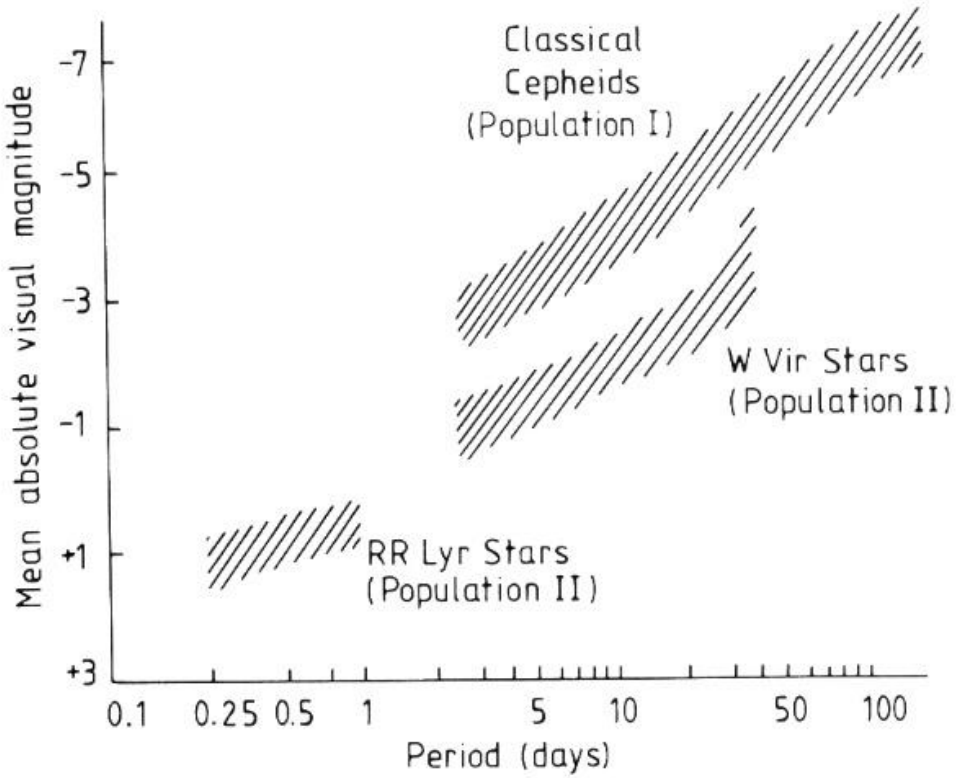

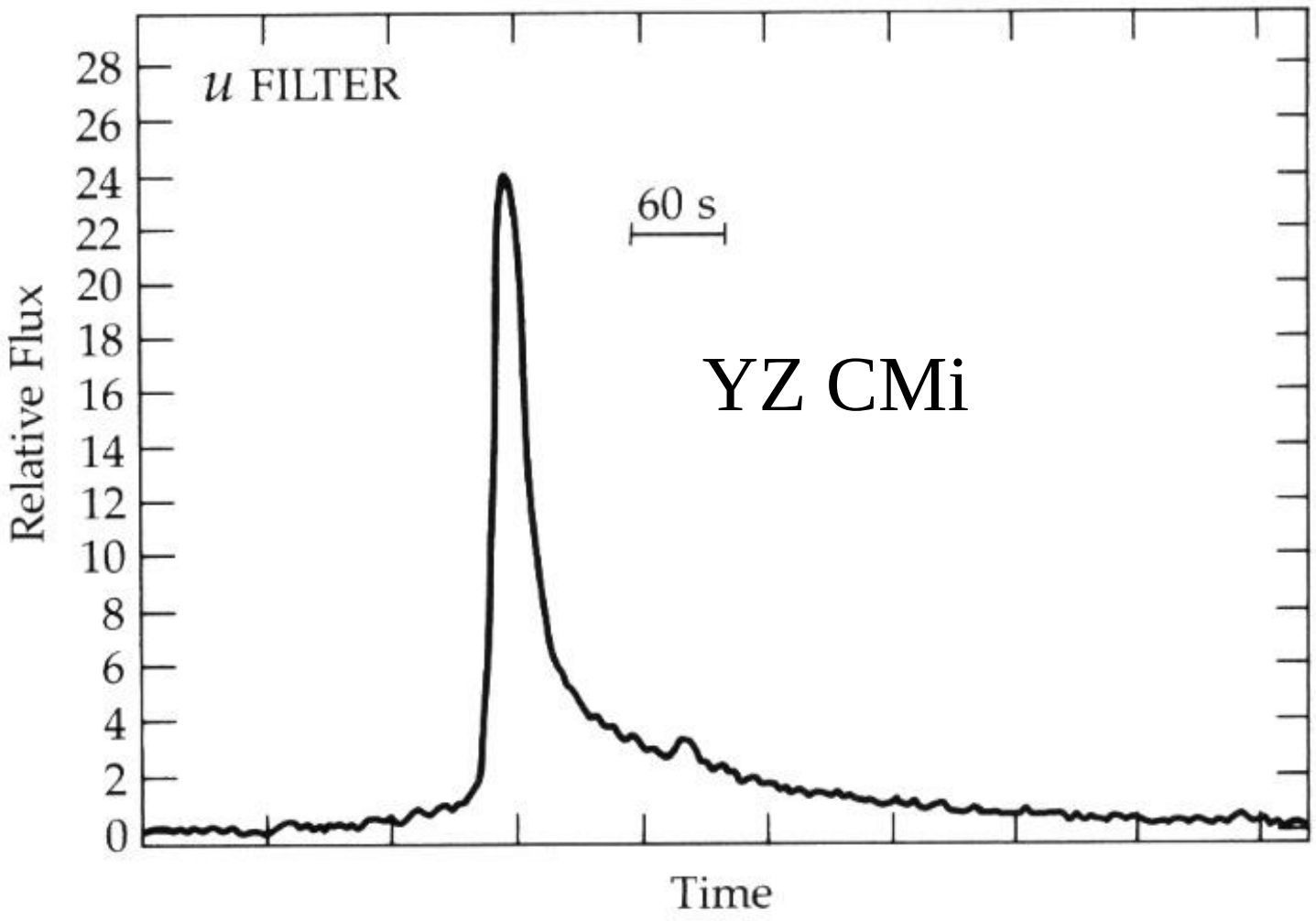

A stellar flare from an M dwarf

Moffett (1974)

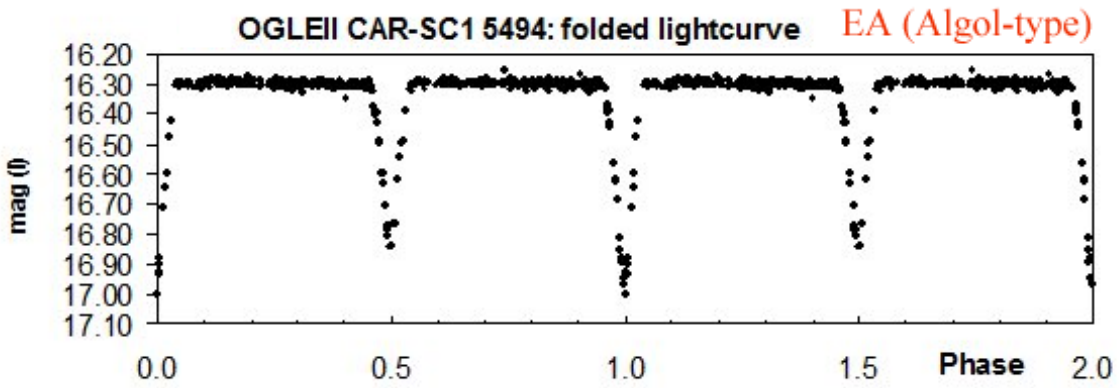

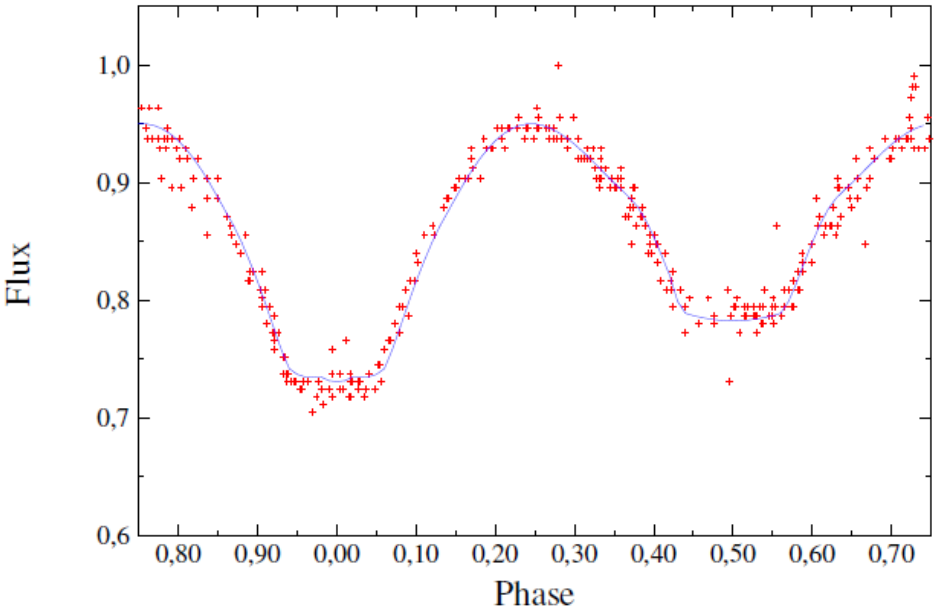

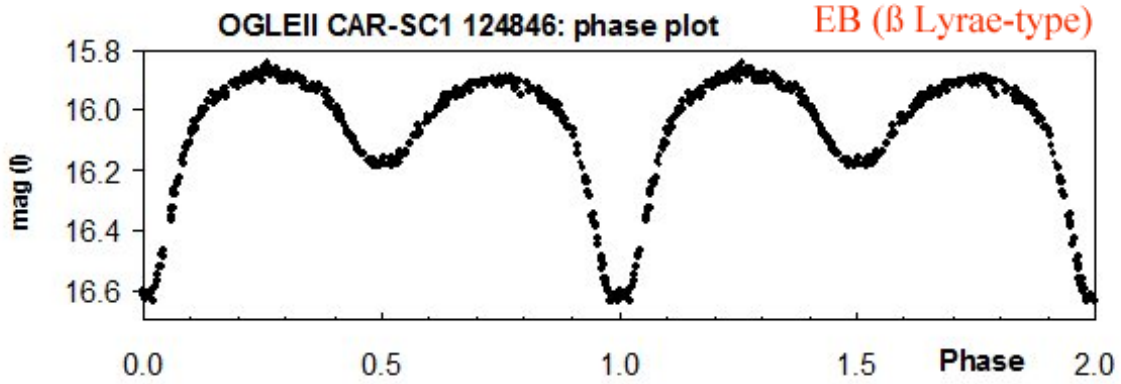

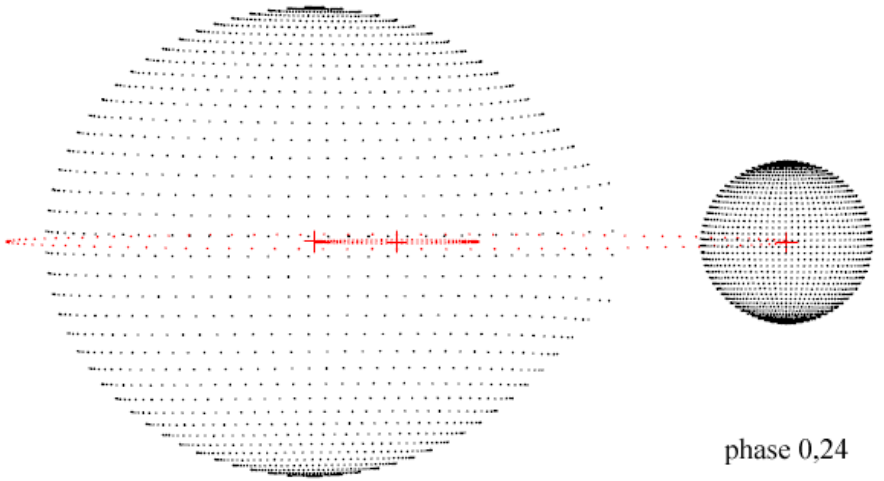

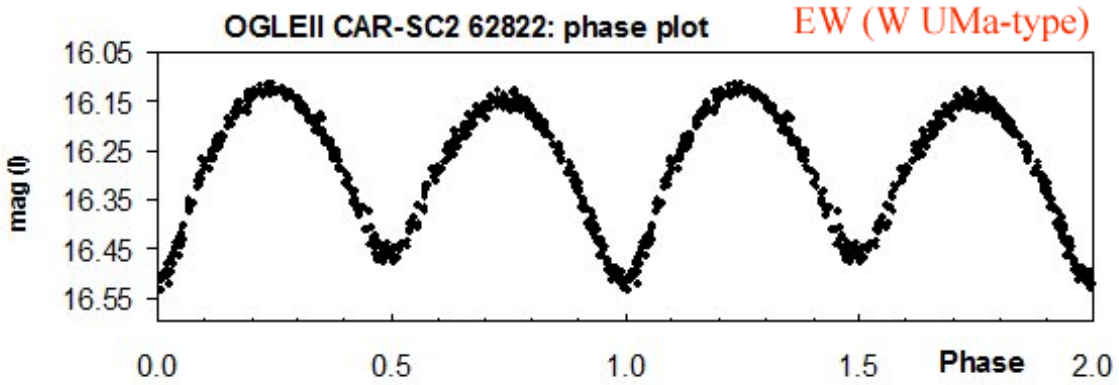

https://vs-compas.belastro.net/bulletin/issue/2/p6